



# Seasonal and Spatial Variation of Groundwater Quality Vulnerable Zones of Yellareddygudem Watershed, Nalgonda District, Telangana State, India

N. Subba Rao<sup>1</sup> · A. Dinakar<sup>1</sup> · B. Karuna Kumari<sup>2</sup> · D. Karunanidhi<sup>3</sup> · T. Kamalesh<sup>1</sup>

Received: 3 July 2020 / Accepted: 1 November 2020 / Published online: 24 November 2020  
© Springer Science+Business Media, LLC, part of Springer Nature 2020

## Abstract

Evaluation of seasonal and spatial variations in vulnerable zones for poor groundwater quality is essential for the protection of human health and to maintain the crop yields. With this objective, groundwater samples were collected seasonally (i.e., pre- and post-monsoon) from the Yellareddygudem watershed of Telangana, India. These samples were analysed for major chemical parameters (pH, TDS,  $\text{Ca}^{2+}$ ,  $\text{Mg}^{2+}$ ,  $\text{Na}^+$ ,  $\text{K}^+$ ,  $\text{HCO}_3^-$ ,  $\text{Cl}^-$ ,  $\text{SO}_4^{2-}$ ,  $\text{NO}_3^-$ , and  $\text{F}^-$ ). Geographical information system (GIS) tools were used to delineate the seasonal and spatial variations for vulnerable zones related to the drinking groundwater quality index (DGQI) and irrigation groundwater quality index (IGQI). Geochemical facies and relations, Piper diagrams, and principal component analysis indicated that the weathering, dissolution, leaching, ion exchange, and evaporation were the primary processes controlling the groundwater quality seasonally. Human influences were the secondary factors. The TDS,  $\text{Na}^+$ ,  $\text{K}^+$ ,  $\text{Cl}^-$ ,  $\text{SO}_4^{2-}$ , and  $\text{F}^-$  parameters were observed to be within the drinking water quality standard limits in most post-monsoon groundwater samples. However, the DGQI showed an increase in the number of samples with unsuitable quality for drinking in the post-monsoon period compared with the pre-monsoon period. The IGQI demonstrated that the number of samples with unsuitable quality for irrigation increased in the post-monsoon period compared to the pre-monsoon period. The differences in the vulnerable zones between the pre- and post-monsoon periods were due to variations in groundwater recharge, following the topography. Thus, the present study will help decision makers to plan groundwater treatment measures within vulnerable zones.

For development of economy and improvement of human health, the groundwater resources play a significant role (Zhou et al. 2016; Li et al. 2017). Generally, the groundwater is not easily contaminated compared with the surface water. However, once the groundwater is polluted, it is very difficult to remediate the contaminated resource (Li et al. 2019a, 2019b; Lu et al. 2019; Wang et al. 2020). Because of the continuous groundwater exploitation and anthropogenic activities, geoenvironmental issues can occur (Subba Rao

et al. 2012a, 2012b, 2020a; Zhang et al. 2018; He and Wu 2019a, 2019b; Wu et al. 2019; Su et al. 2020; Subba Rao 2020). Therefore, it is an important aspect to enhance the hydrogeological research for sustainable economic development of any area.

Due to rapid population growth and industrialization, there has been an incredible increase in the demand for drinking water, which directly affects the human health and crop growth (Li and Qian 2018; Li 2020). Therefore, a number of researchers have been focused on the chemical quality of groundwater from the different parts of the world (Kumar et al. 2010; Li et al. 2018a, 2018b; Subba Rao 2018; Ji et al. 2020). For instance, Yidana and Yidana (2010) evaluated the groundwater chemistry in Ghana, utilizing water quality index and multivariate analysis, and observed that the rock weathering and cation exchange were the most important processes controlling the groundwater chemistry and noted that the groundwater quality was suitable for drinking purpose. Subba Rao et al. (2012b) assessed the chemical quality of groundwater, which was not suitable for drinking,

✉ N. Subba Rao  
srnandipati@gmail.com

<sup>1</sup> Department of Geology, Andhra University,  
Visakhapatnam 530 003, India

<sup>2</sup> Anuhya Architects, Sreeramnagar Colony,  
Hyderabad 500 050, India

<sup>3</sup> Department of Civil Engineering, Sri Shakthi Institute  
of Engineering and Technology (Autonomous),  
Coimbatore 641 062, India

irrigation, and industrial uses in most part of the Varaha River basin, Visakhapatnam district, Andhra Pradesh, India. Krishnakumar et al. (2014) conducted a study on the groundwater quality in and around Vedaraniyam, Tamilnadu, India, and found that the inferior chemical quality of groundwater was caused by uncontrolled usage of pesticides in the agricultural fields. El Alfy et al. (2015) extensively studied the chemical quality of groundwater from the arid regions of Saudi Arabia and observed that the deterioration of groundwater quality was caused by minerals dissolution, evaporation, and human activities. Venkatramanan et al. (2016) assessed the quality of groundwater, using geographical information system (GIS) and water quality index from Thiruthuraiipoondi City in Cauvery deltaic region, Tamil Nadu, India, and observed that the contamination of groundwater was a consequence of waste water irrigation and sea water incursion and noted that the groundwater quality was unfit in certain parts for drinking and agricultural purposes. Sener et al. (2017) evaluated the groundwater quality, using water quality index and GIS, in Aksu river, Southwest Turkey and found that the groundwater quality was poor and very poor types due to dominance of pollution activities. Ayadi et al. (2018) examined the geochemistry and groundwater quality from the Northwestern Tunisia and found that the silicate weathering and mineral dissolution, carbonate dissolution, ion-exchange and anthropogenic contamination were the important factors, governing the chemistry, and quality of groundwater. Deepali et al. (2019) evaluated the groundwater quality and human health risk from a semi-arid region of eastern Maharashtra, India, and observed that the water–rock interactions, dedolomitization, and reverse ion exchange were the controlling processes of the groundwater quality and also noted that the groundwater quality was not suitable for drinking in some groundwater samples. Omonona et al. (2019) studied the hydrochemical characteristics and groundwater quality from the Southeastern Nigeria and found that the chemistry of groundwater was mainly influenced by silicate and carbonate weathering, and ion exchange factors, and noted that the groundwater quality was not suitable for irrigation purpose. Ji et al. (2020) conducted a survey on the seasonal characteristics of water quality for domestic purpose in Hancheng City of the Guanzhong plain, China, and observed that the most water samples were of good quality for drinking and domestic purposes. Ramachandran et al. (2020) evaluated the seasonal drinking groundwater quality based on the water-quality index and GIS in Adyar River basin, Chennai, Tamilnadu, India, and found that the groundwater quality was not suitable for drinking in most of the study region. Zhou et al. (2020) examined the hydrogeochemistry and nature of groundwater quality for drinking and irrigation purposes from Xinle City, North China, and found that the industrial and agricultural activities were the main factors, causing the contamination

of groundwater and also noted that the groundwater quality was not suitable for drinking and irrigation purposes.

In Telangana State, India, most of the groundwater studies were focused on the general groundwater quality and fluoride contamination (Brindha et al. 2011; Subba Rao et al. 2016, 2018, 2020b; Narsimha 2020a, 2020b), but not on the seasonal and spatial variation of groundwater quality, using drinking groundwater quality index (DGQI), irrigation groundwater quality index (IGQI), and geographical information system (GIS). In view of this, the present study area of Yellareddygudem watershed had been chosen from a part of Nalgonda district, Telangana State. The main objective of the present study was to delineate the seasonal and spatial distribution of groundwater quality vulnerable zones, using DGQI, IGQI, and GIS techniques. This study is significant for research in groundwater quality and will help to recognize the groundwater quality vulnerable zones seasonally and spatially for implementing the suitable remedial measures by civic authorities.

## Materials and Methods

### Study Area

Geographically, the present study area of Yellareddygudem watershed, lying between latitude 17°09′–17°21′N and longitude 79°13′–79°26′E, is located in Nalgonda district, Telangana State, India (Fig. 1), covering an area of 79 km<sup>2</sup>. It experiences dry climate. The average annual temperature is in between 17.6 °C in winter starting from December to February and 40 °C in summer starting from March to May. The average annual rainfall is about 750 mm. Approximately 70% (525 mm) of the rainfall comes from the southwest monsoon (June to September), 22% (165 mm) from the northeast monsoon (October to November), and the rest 8% (60 mm) from the non-monsoon (December to May). The potential evapotranspiration is approximately 1350 mm (CGWB 2015). The drainage pattern is sub-dendritic type.

### Geology

Topographically, the elevation of the present study area is from 360 m above mean sea level (amsl) in the northwestern part to 240 m amsl in the southeastern part (Fig. 1), with an average topographic gradient of approximately 3 m/km. Black soils are the dominant soil type. The depth of soil cover is from 1 to 2 m from the ground surface. The calcium carbonate concretion (locally called *kankar*) occur in the soil zone, which is a characteristic feature of dry climate. The present study area is underlined by granite rocks of the Archaean age. The rocks contain the pink and grey varieties with younger intrusive bodies (dolerite and quartzite), which

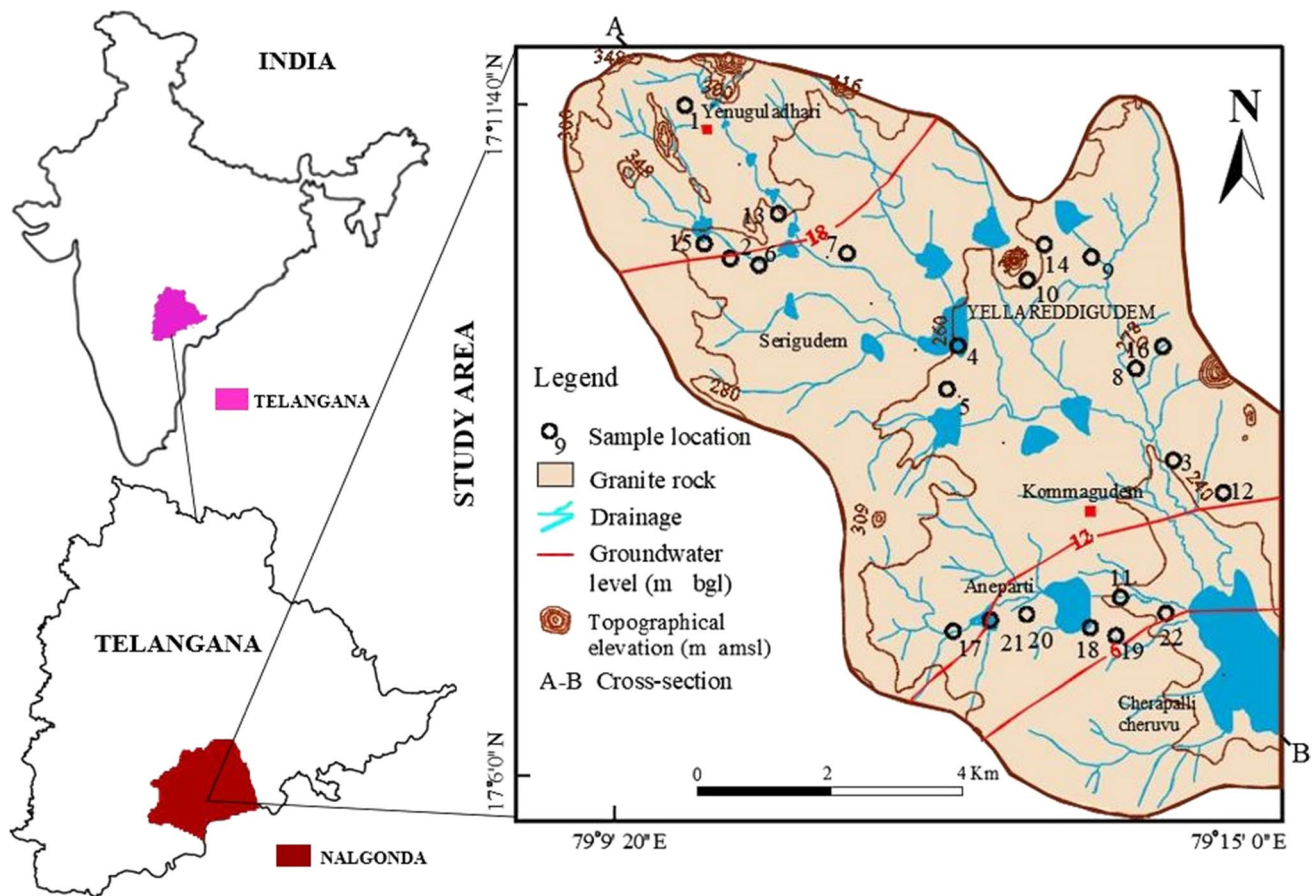


Fig. 1 Location of the study area, Yellareddygudem watershed of Telangana, India

have the minerals of quartz, feldspar, biotite, hornblende, fluorite, and apatite. They show the N–S or E–W orientation with a dip of  $55^{\circ}$  to  $70^{\circ}$  southeast.

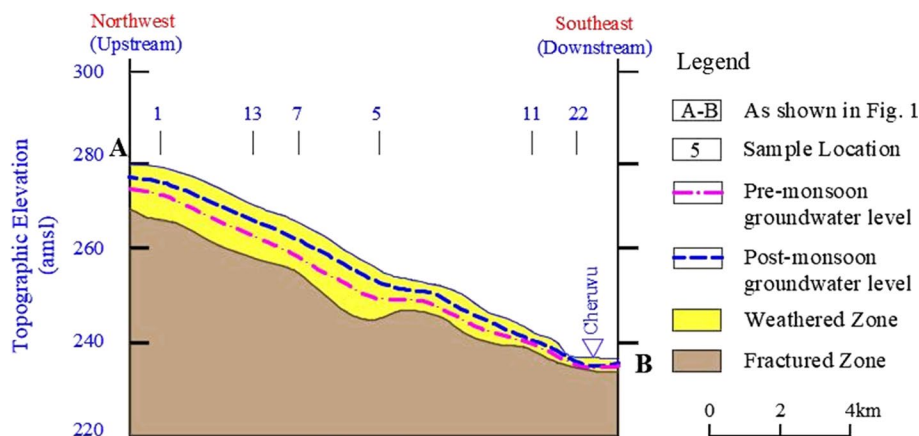
### Hydrogeology

Seasonal rainfall is the principle recharge source of the groundwater (Ji et al. 2020). Irrigation-return-flows are the secondary source of the groundwater recharge (Subba Rao et al. 2017). Withdrawal of groundwater is mainly through bore wells. The rocks present in the study area have limited primary porosity. However, they become the water-bearing formations (aquifers) due to development of secondary porosity (weathered activity and tectonic process). The groundwater exists in the weathered zone (4–27 m) under the unconfined aquifer conditions and in the fractured zone (13–87) under the semiconfined aquifer conditions. The depth to groundwater table is from approximately 6–18 m below ground level (bgl) in the pre-monsoon period and 4–14 m bgl in the post-monsoon period, being deeper in the upstream side (northwestern part) and shallower in the

downstream side (southeastern part), which follows the topography (Fig. 1).

The cross-section of the hydrogeological conditions (aquifer structure) drawn from the direction of northwestern to southeastern sides is shown in Figs. 1 and 2. The depth of soil cover varies from 1 to 1.5 m from the ground surface. It results from the highly weathering activity in the upper part of the country rock, which reduces the hydraulic conductivity to some extent. The soil cover is followed by the weathering rock portion, which depth varies from 1.5 to 15.8 m. It is characterized by low hydraulic conductivity due to a limited pore spaces to allow the water flow within it. The weathered zone is followed by the fractured rock portion. It has the depth from 12.6 to 51.5 m, which shows the high hydraulic conductivity due to development of continuous connection of pore spaces in it to allow the water flow freely from one pore space to another one. Finally, the massive rock portion occurs, following the fractured rock portion. The depth to groundwater level varies from approximately 3–9 m bgl in the pre-monsoon period and is from 2 to 5 m bgl in the post-monsoon period, being deeper in the northwestern side (upstream), which is a recharge area, and lower

**Fig. 2** Cross-section of hydro-geological conditions



in the southeastern side (downstream), which is a discharge area, following the topographical features.

The quality of groundwater is not potable due to its brackish type in most part of the study area. In some locations, the health problems, such as discoloration of teeth and fluorosis, are observed during the field work due to consumption of fluoride contaminated groundwater. This may be caused by occurrence of the fluoride-bearing minerals (biotite, hornblende and apatite) in the country rocks.

#### Land Use/Land Cover

Approximately 64% of the present study area is covered by irrigated land, 22% by built-up land, 12% by waste land, and 2% by surface water bodies and streams. Agricultural activities are intensive and long-term practice and unlimited utilization of chemical fertilizers is the most common for higher crop output. Rice, cotton, and pulses are the important commercial crops. Poor drainage conditions (dumping of household wastes, leakage of wastewater channels, spillage of septic tanks, etc.) are very common.

#### Groundwater Sampling and Chemical Analysis

A total of 44 groundwater samples (22 in each season) were collected from the present study area in the pre- and post-monsoon periods 2015 (Fig. 1), which are confined to unconfined to semi-confined aquifer conditions. They are used for both domestic and irrigation purposes. Before collecting the groundwater samples from the wells, the wells were pumped for two to three times to eliminate the influence of stagnant water. The groundwater samples were collected in half litre polyethylene containers. The containers were soaked in 1:1 HCl for 24 h and then they were rinsed with distilled water, following the deionized water. After collecting the groundwater samples, they were labeled, stored, and transported to the laboratory for chemical analysis.

The groundwater samples were analysed for chemical parameters, including hydrogen-ion-concentration (pH), electrical conductivity (EC), total dissolved solids (TDS), calcium ( $\text{Ca}^{2+}$ ), magnesium ( $\text{Mg}^{2+}$ ), sodium ( $\text{Na}^+$ ), potassium ( $\text{K}^+$ ), bicarbonate ( $\text{HCO}_3^-$ ), chloride ( $\text{Cl}^-$ ), sulphate ( $\text{SO}_4^{2-}$ ), nitrate ( $\text{NO}_3^-$ ), and fluoride ( $\text{F}^-$ ), following the standard chemical water quality procedures of American Public Health Association (APHA 2012). The chemical analysis of water was performed, following the duplicate analyses procedure. The groundwater samples were determined for the chemical parameters at Regional Chemical Laboratory, Central Ground Water Board, Southern Region, Hyderabad, India.

The pH and EC were measured, using their meters (Hanna HI 9811-5). The EC was used to compute the TDS ( $\text{EC} \times 0.65$ ), as suggested by Hem (1991). The TA and  $\text{HCO}_3^-$  were estimated by HCl titrimetric method. The TH and  $\text{Ca}^{2+}$  were analysed by EDTA volumetric method. The  $\text{Mg}^{2+}$  was calculated, taking the difference value between TH and  $\text{Ca}^{2+}$ . The ions  $\text{Na}^+$  and  $\text{K}^+$  were determined by flame photometer (Systronics 130 make). The  $\text{Cl}^-$  was measured, using  $\text{AgNO}_3^-$  titrimetric method. The  $\text{SO}_4^{2-}$  was estimated, using UV–visibile spectrophotometer procedure (Systronics 135 make), the  $\text{NO}_3^-$ , using colorimetric method (Systronics 112 make) and the  $\text{F}^-$ , using specific ion analyser (Orion make). The units of the chemical parameters were expressed in milligrams per litre (mg/L) and milliequivalent per litre (meq/L), except pH (nondimensional) and EC ( $\mu\text{S}/\text{cm}$  at 25 °C).

The concentrations of cations ( $\sum\text{CC}$ ;  $\text{Ca}^{2+}$ ,  $\text{Mg}^{2+}$ ,  $\text{Na}^+$  and  $\text{K}^+$ ) and anions ( $\sum\text{CA}$ ;  $\text{HCO}_3^-$ ,  $\text{Cl}^-$ ,  $\text{SO}_4^{2-}$ ,  $\text{NO}_3^-$ , and  $\text{F}^-$ ) expressed in meq/L of each groundwater sample were computed for checking the accuracy of the analysed results, using ionic balance error (IBE), as shown in Eq. 1. This is expressed in percentage (%). The computed IBE was within the standard limit of  $\pm 5\%$  (Subba Rao 2017), which indicates the reliability of the analysed results.



$$IBE = \frac{\sum CC - \sum CA}{\sum CC + \sum CA} \times 100 \quad (1) \quad Q_R = \frac{C}{D} \times 100 \quad (3)$$

### Drinking Groundwater Quality Index

To assess the overall groundwater quality in terms of drinking groundwater quality index (DGQI), the chemical parameters, such as pH, TDS,  $Ca^{2+}$ ,  $Mg^{2+}$ ,  $Na^+$ ,  $K^+$ ,  $HCO_3^-$ ,  $Cl^-$ ,  $SO_4^{2-}$ ,  $NO_3^-$  and  $F^-$ , were used. This is a single digital platform to indicate the comprehensive water quality type (Subba Rao et al. 2020b). For the computation of DGQI, five steps were involved. In the first step, the unit weight ( $U_w$ ) was assigned for every chemical parameter ( $i$ ), depending upon its relative importance on human health. For instance, the most significant parameter had a weight of 5 and the lowest significant had a weight of 1 (Table 1). In the second step, the relative weight ( $R_w$ ) was calculated for every chemical parameter (Eq. 2). In the third step, the percentage of quality rating scale ( $Q_R$ ) was computed by dividing the concentration of chemical parameter ( $C$ ) with its standard drinking water quality ( $D$ ) for every chemical parameter (Eq. 3). In the fourth step, the relative rating ( $R_R$ ) was quantified by multiplying  $R_w$  with  $Q_R$  in each chemical parameter (Eq. 4). In the final step, the DGQI was computed by adding all  $R_R$  in each sample (Eq. 5).

$$R_w = \frac{U_w}{\sum_{i=1}^n U_w} \quad (2)$$

**Table 1** Particulars of desirable limits ( $D$ ), unit weight ( $U_w$ ) and relative weight ( $R_w$ ) for drinking purpose

Chemical parameters	$D$	$U_w$	$R_w$	References
pH	8.5	4	0.100	BIS (2012) and WHO (2017)
TDS (mg/L)	500	5	0.125	BIS (2012) and WHO (2017)
$Ca^{2+}$ (mg/L)	75	2	0.050	BIS (2012) and WHO (2017)
$Mg^{2+}$ (mg/L)	30	2	0.050	BIS (2012) and WHO (2017)
$Na^+$ (mg/L)	200	4	0.100	BIS (2012) and WHO (2017)
$K^+$ (mg/L)	12	2	0.050	Subba Rao et al. (2019)
$HCO_3^-$ (mg/L)	300	1	0.025	BIS (2012) and WHO (2017)
$Cl^-$ (mg/L)	250	5	0.125	BIS (2012) and WHO (2017)
$SO_4^{2-}$ (mg/L)	200	5	0.125	BIS (2012), WHO (2017)
$NO_3^-$ (mg/L)	45	5	0.125	BIS (2012)
$F^-$ (mg/L)	1.5	5	0.125	BIS (2012)
Total		$\sum 40$	$\sum 1.00$	

$$R_R = R_w \times Q_R \quad (4)$$

$$DGQI = \sum R_R \quad (5)$$

### Irrigation Groundwater Quality Index

Suitability of the chemical quality of groundwater for irrigation purpose depends on the degree of salinity (EC), percent sodium (% $Na^+$ ), sodium adsorption ratio (SAR), residual sodium carbonate (RSC), permeability index (PI), magnesium ratio (MR), and Kelly's ratio (KR), as suggested by Kelley (1940), Eaton (1950), USSL (1954), Wilcox (1955), Doneen (1964), Szabolcs and Darab (1964), in addition to pH and  $SO_4^{2-}$ , which also were widely used (Subba Rao et al. 2012a, 2012b; Subba Rao 2017, 2018). They were computed, as shown below (Eqs. 6 and 11), taking the ions in meq/L.

$$SAR = \frac{Na^+}{\sqrt{\frac{(Ca^{2+} + Mg^{2+})}{2}}} \quad (6)$$

$$\%Na^+ = \left[ \frac{(Na^+ + K^+)}{(Ca^{2+} + Mg^{2+} + Na^+ + K^+)} \right] \times 100 \quad (7)$$

$$RSC = (HCO_3^- + CO_3^{2-}) - (Ca^{2+} + Mg^{2+}) \quad (8)$$

$$PI = \frac{Na^{2+} \sqrt{HCO_3^-}}{(Ca^{2+} + Mg^{2+} + Na^{2+})} \times 100 \quad (9)$$

$$MR = \frac{Mg^{2+}}{(Ca^{2+} + Mg^{2+})} \times 100 \quad (10)$$

$$KR = \frac{Na^+}{(Ca^{2+} + Mg^{2+})} \quad (11)$$

The irrigation groundwater quality index (IGQI) was computed (Eq. 12), considering the irrigation water quality limits of pH, EC,  $SO_4^{2-}$ , SAR, % $Na$ , RSC, PI, MR, and KR into account (Table 2), on par with the calculation procedure of DGQI (Eqs. 2 and 5).

$$IGQI = \sum R_R \quad (12)$$

**Table 2** Particulars of desirable limits ( $D$ ), unit weight ( $U_w$ ) and relative weight ( $R_w$ ) for irrigation purpose

Chemical parameter	$D$	$U_w$	$R_w$	References
pH	8.5	1	0.037	BIS (2012)
EC ( $\mu\text{S}/\text{cm}$ )	1500	2	0.074	Freeze and Cherry (1979)
$\text{SO}_4^{2-}$ (mg/L)	400	4	0.148	Dinakar (2018)
SAR	18	3	0.111	USSL (1954)
% $\text{Na}^+$	60	4	0.148	Wilcox (1955)
RSC (meq/L)	2.5	3	0.111	Eaton (1950)
PI (meq/L)	75	3	0.111	Domenico and Schwartz (1990)
MR (meq/L)	50	2	0.074	Szaboles and Darab (1964)
KR (meq/L)	1	5	0.185	Kelly (1957)
Total		$\sum 27$	$\sum 1.000$	

## Geographical Information System (GIS) Analysis

Geographical information system (GIS) is a tool to delineate the spatial distribution of groundwater quality (Karunanidhi et al. 2020). ArcGIS software was used here to plot the spatial distribution of values of drinking groundwater quality index (DGQI) and irrigation groundwater quality index (IGQI), using inverse distance weighted interpolation technique (Karunanidhi et al. 2020) for identifying the vulnerable zones for protection and management of groundwater resources.

## Results and Discussion

### Generalized Quality of Groundwater

Statistical summary (minimum, maximum, arithmetic mean, standard deviation, and coefficient of variation) of the seasonal variation of physical parameters (pH, EC, and TDS), major cations ( $\text{Ca}^{2+}$ ,  $\text{Mg}^{2+}$ ,  $\text{Na}^+$ , and  $\text{K}^+$ ), and major anions ( $\text{HCO}_3^-$ ,  $\text{SO}_4^{2-}$ ,  $\text{Cl}^-$ ,  $\text{NO}_3^-$ , and  $\text{F}^-$ ) are shown in Table 3. They were used to evaluate the influence of individual chemical parameter on human health and agricultural products through the consumption of groundwater for drinking and irrigation purposes.

**Table 3** Statistical summary of seasonal chemical composition of groundwater

Particulars	Pre-monsoon period (Pre)		Post-monsoon period (Post)		Arithmetic mean		Standard deviation		Coefficient of variation (%)		Ionic contribution (%)	
	Min	Max	Min	Max	Pre	Post	Pre	Post	Pre	Post	Pre	Post
Physical parameters												
pH	6.21	8.03	6.74	9.25	7.15	7.62	0.39	0.53	5.45	7.00	–	–
EC ( $\mu\text{S}/\text{cm}$ )	443.00	5900.00	291.00	5744.00	2085.00	1926.00	1264.99	1213.8	60.67	63.01	–	–
TDS (mg/L)	128.50	3835.00	208.00	3698.00	1355.21	1318.00	822.20	831.83	60.67	63.13	–	–
Major cations												
$\text{Ca}^{2+}$ (mg/L)	18.00	240.00	26.00	281.00	92.55	134.00	51.81	70.34	55.98	52.69	23.88	30.40
$\text{Mg}^{2+}$ (mg/L)	3.60	112.00	5.00	248.00	39.60	66.00	28.65	56.80	72.34	85.78	16.85	24.67
$\text{Na}^+$ (mg/L)	49.00	689.00	22.00	700.00	255.32	223.00	163.59	173.28	64.07	77.72	57.42	44.07
$\text{K}^+$ (mg/L)	0.48	89.70	1.00	30.00	14.14	7.30	20.16	6.30	142.57	87.00	1.85	0.86
Major anions												
$\text{HCO}_3^-$ (mg/L)	140.00	1000.00	159.00	1129.00	607.00	535.00	183.84	205.00	30.29	38.32	47.56	41.29
$\text{Cl}^-$ (mg/L)	35.00	808.00	21.00	766.00	252.68	256.00	213.18	192.60	84.37	75.31	34.08	33.99
$\text{SO}_4^{2-}$ (mg/L)	0.58	403.00	3.00	376.00	106.28	93.00	120.49	107.20	113.37	114.80	10.56	9.13
$\text{NO}_3^-$ (mg/L)	1.20	719.00	2.00	700.00	90.70	199.60	182.30	226.90	201.08	113.70	6.98	15.16
$\text{F}^-$ (mg/L)	0.42	7.50	0.27	4.73	3.23	1.72	2.31	1.48	71.52	85.92	0.82	0.43

### Physical Parameters of Groundwater Quality

The physical parameters of the groundwater include the hydrogen-ion-concentration (pH), electrical conductivity (EC), and total dissolved solids (TDS). The results of the physical parameters are presented in Table 3 and Fig. 3. The pH varied from 6.21 to 9.25 with a mean value of 7.15 in the pre-monsoon period and 7.62 in the post-monsoon period (Table 3; Fig. 3), indicating alkaline condition of groundwater. The pH of 68.18% of the groundwater samples (4–7, 9, 10, 13–20, and 22) were more than 7.0. These groundwater samples were distributed in the entire study area (Fig. 1). The pH for other 31.82% of the groundwater samples (1, 2, 3, 8, 11, 12, and 21) was in between 6.21 and 6.90, which was located in the northwestern, eastern, and southern side in both the seasons. According to the standard drinking water quality limit of pH (6.5–8.5) recommended by (BIS 2012; WHO 2017), the pH of 95.45% of the groundwater samples in the pre- (2–22) and post-monsoon (1–11 and

13–22) periods was within this limit. Besides, the high pH of irrigation water (> 8.5), which is harmful to plants, may be caused by high concentrations of  $\text{HCO}_3^-$  and  $\text{CO}_3^{2-}$ . They lead  $\text{Ca}^{2+}$  and  $\text{Mg}^{2+}$  ions to form insoluble minerals leaving  $\text{Na}^+$  as the predominant ion in solution, which decreases the water flow rate (Bauder et al. 2014).

The EC, which is an ability to conduct current of the salts, ranged from 291 to 5900  $\mu\text{S}/\text{cm}$ , with a mean value of 2085 and 1926  $\mu\text{S}/\text{cm}$  in the pre- and post-monsoon groundwater samples, respectively (Table 3; Fig. 3). It demonstrates a wide variation in the activities of geochemical processes. As per the classification of EC (Subba Rao et al. 2012b), 40.91% of the groundwater samples (1, 2, 5, 13, 15, 17, 18, 20, and 22) were determined as Type I (EC: < 1500  $\mu\text{S}/\text{cm}$ ), 45.45% of the groundwater samples (3, 4, 6, 7, 10 to 12, 16, 19, and 21) as Type II (EC: 1500–3000  $\mu\text{S}/\text{cm}$ ) and 13.64% of the groundwater samples (8, 9, and 14) as Type III (EC: > 3000  $\mu\text{S}/\text{cm}$ ) in the pre-monsoon period, and 31.82% of the groundwater samples (1, 5, 12, 14, 15, 17, and 22) as Type I, 50% of the groundwater samples (2, 6, 7, 10, 11, 13, 16, 18, 19, 20, and 21) as Type II and 18.18% of the groundwater samples (3, 4, 8, and 14) as Type III in the post-monsoon period (Fig. 1). They represented the low, medium, and high enrichment of salts, respectively. Generally, Type I is a result of lithological source (water–rock interactions), whereas Type III is caused by nonlithological source (anthropogenic), such as household wastewaters, spillages of septic tanks, irrigation-return-flows, and chemical fertilizers (Subba Rao 2017). Type II may be considered as a transition type between Type I and Type III. The decrease of a number of groundwater samples in Type I from the pre- to post-monsoon periods, whereas the increase of a number of groundwater samples in Type II and Type III from the pre- to post-monsoon periods indicates the enrichment of salts content in the post-monsoon period due to leaching activity, depending on the influence of water–rock interactions and anthropogenic activities. They enhance the salts in the drinking water, causing the potential health risks. On the other hand, the primary impact of high EC (salinity hazard) water on crop yield is the inability of the plant to imbibe water (physiological drought). So, the higher the EC, the lesser is the water availability to plants (Bauder et al. 2014).

A total salt content dissolved in the water is expressed in terms of total dissolved solids (TDS). It ranged from 128.50 to 3835 mg/L, with a mean value of 1355.21 and 1318 mg/L in the pre- and post-monsoon periods, respectively (Table 3; Fig. 3). It reflects a lot of variation in the groundwater salinity due to involvement of various chemical processes (Subba Rao 2020). According to the range of TDS (Subba Rao 2017), 40.91% of the pre-monsoon groundwater samples (1, 2, 5, 13, 15, 17, 18, 20, and 22) and 54.55% of the post-monsoon groundwater samples (1, 5 to 7, 11, 12, 14, 15, 17, 19, 21, and 22) were classified as

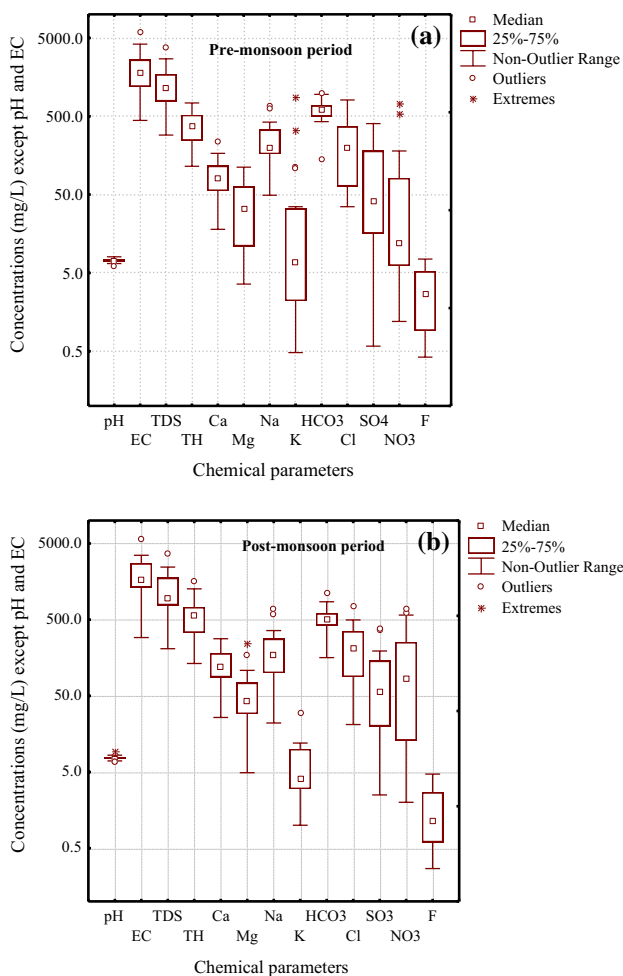


**Fig. 3** Box plot showing the chemical composition of groundwater of the pre-monsoon period (a) and post-monsoon period (b)

fresh water category (TDS: < 1000 mg/L) due to influence of geogenic origin. The other groundwater samples (59.09% in the pre-monsoon period and 45.45% in the post-monsoon period) were brackish category (TDS: 1000–10,000 mg/L) caused by impact of anthropogenic source on the groundwater system. Compared with the desirable standard limit of TDS (500 mg/L) for consumable potable water, 95.45% of the pre-monsoon groundwater samples (2–22) exceeded the TDS by 1.15–7.67 times, and 81.82% of the post-monsoon groundwater samples (2–13 and 16–21) exceeded the TDS by 1.05–7.40 times, causing the stomach irritation (BIS 2012; WHO 2017).

### Major Cations of Groundwater Quality

The calcium ( $\text{Ca}^{2+}$ ), magnesium ( $\text{Mg}^{2+}$ ), sodium ( $\text{Na}^+$ ), and potassium ( $\text{K}^+$ ) ions come under the major cations. The analytical results of the cations of the groundwater samples are shown in Table 3. The  $\text{Ca}^{2+}$  is a key element in many geochemical processes, which releases from the weathering of calcium feldspar, amphibole, apatite, and fluorite minerals into the groundwater body (Subba Rao 2017). In the groundwater of the present study area, the  $\text{Ca}^{2+}$  content varied from 18 to 281 mg/L with mean values of 92.55 and 134 mg/L in the pre- and post-monsoon periods, respectively (Fig. 3). The contribution of  $\text{Ca}^{2+}$  to the total cations was 23.88% and 30.40% in the pre- and post-monsoon groundwater samples (Table 3). The drinking water quality standard limit of  $\text{Ca}^{2+}$  is 75 mg/L (BIS 2012), which exceeded in 68.18% of the pre-monsoon groundwater samples (2, 6, 8, 9, 11–16, and 18–22) and 77.27% of the post-monsoon groundwater samples (2–10, 13–18, 20, and 21; Fig. 1). The respective concentrations were 1.04–3.20 and 1.17–3.75 times higher than their recommended limits for drinking purpose. It develops scale formation (WHO 2017). The  $\text{Ca}^{2+}$  plays a significant role to reduce the  $\text{Na}^+$  content in the soil water, and thereby it increases the soil permeability. It assists in planting development through the effectively water circulation (Bauder et al. 2014).

Ferromagnesium minerals (biotite and hornblende) and domestic waste waters are the main sources of  $\text{Mg}^{2+}$  in the groundwater (Subba Rao 2017). In the present study area, the  $\text{Mg}^{2+}$  was from 3.6 to 248 mg/L in the pre- and post-monsoon groundwater samples with a mean value of 39.60 and 66 mg/L, respectively (Table 3; Fig. 3). The  $\text{Mg}^{2+}$  contribution to the total cations was 16.85% and 24.67% in the pre- and post-monsoon periods, respectively (Table 3). As per the drinking water quality standards, the  $\text{Mg}^{2+}$  should not exceed 30 mg/L in the water (BIS 2012). However, it was 1.07–3.73 and 1.37–8.27 times more than the desirable limit in 59.09% of the pre-monsoon groundwater samples (3–11, 13, 14, 15, and 21) and 68.18% of the post-monsoon groundwater samples (2–5, 7–13, 16, 18, 20, and 22; Fig. 1). It

forms scale formation (WHO 2017). In addition, the higher amount of  $\text{Mg}^{2+}$  in the irrigated water supports the plant take-up of  $\text{Ca}^{2+}$  or  $\text{K}^+$ , which causes their lacks in plant tissue (Franklin et al. 2008; Bauder et al. 2014).

The concentration of  $\text{Na}^+$  was in between 22 and 700, with a mean value of 255.32 and 223 mg/L in the pre- and post-monsoon periods, respectively (Table 3; Fig. 3). It is derived from the plagioclase feldspars (Subba Rao 2017). Poor drainage conditions are the additional source of  $\text{Na}^+$  in the groundwater (Subba Rao et al. 2017). The  $\text{Na}^+$  contributed 57.42% and 44.07% to the total cations in the pre- and post-monsoon groundwater samples, respectively (Table 3). In 45.45% of the pre-monsoon groundwater samples (3, 4, 6, 8, 9, 11, 14, 16, 19, and 21) and 36.36% of the post-monsoon groundwater samples (2 to 4, 8, 9, 16, 19, and 20; Fig. 1), the  $\text{Na}^+$  content was 1.32–3.45 and 1.25–3.50 times greater than the safe limit of 200 mg/L recommended for drinking water (BIS 2012), respectively. It may cause hypertension (WHO 2017). The use of irrigation water with  $\text{Na}^+$  reduces the crop yields under certain soil texture conditions. This condition is called sodicity (Bauder et al. 2014), which is a result of excessive sodium accumulation in the soils. It causes swelling and dispersion of soil clays, surface crusting and pore plugging and thereby obstructs the infiltration of recharge water. This condition reduces the availability of sufficient water. This is the main reason for decline in plants development (Bauder et al. 2014; Subba Rao 2017).

In the present study area, the  $\text{K}^+$  content varied from 0.48 to 89.70 mg/L with a mean value of 14.14 mg/L in the pre-monsoon groundwater and 7.30 mg/L in the post-monsoon groundwater (Table 3; Fig. 3). Orthoclase feldspars and potassium fertilizer are the principle sources of  $\text{K}^+$  in the groundwater (Subba Rao 2017). The  $\text{K}^+$  contributed 1.85% and 0.86% to the total cations in the pre- and post-monsoon periods, respectively (Table 3). The  $\text{K}^+$  content was 1.67–7.48 and 2.5 times greater than the standard limit of 12 mg/L prescribed for potable water (Subba Rao 2017) in 27.27% of the pre-monsoon groundwater samples (8, 9, 11, 14, 18, and 21) and 4.55% of the post-monsoon groundwater samples (2), respectively (Fig. 1). The  $\text{K}^+$  plays a significant role to improve the irrigation water quality for higher crop yields. Without application of  $\text{K}^+$ ,  $\text{K}^+$  fertility of soils will decrease under the long-term cropping. Thus, this is an important element for improvement of irrigation (Li et al. 2013).

### Major Anions of the Groundwater Quality

The major anions, such as bicarbonate ( $\text{HCO}_3^-$ ), chloride ( $\text{Cl}^-$ ), sulphate ( $\text{SO}_4^{2-}$ ), nitrate ( $\text{NO}_3^-$ ), and fluoride ( $\text{F}^-$ ), were analysed from the groundwater samples of the present study area and their results are presented in Table 3. The value of  $\text{HCO}_3^-$  ranged from 140 to 1129 mg/L with a mean



value of 607 and 535 mg/L in the pre- and post-monsoon groundwater samples, respectively (Fig. 3). The  $\text{HCO}_3^-$  is mainly released into the groundwater body due to a result of soil  $\text{CO}_2$ , which originates from the organic decomposition (Subba Rao et al. 2017). The  $\text{HCO}_3^-$  contributed 47.56% and 41.29% to the total anions content in the pre- and post-monsoon periods, respectively (Table 3). The  $\text{HCO}_3^-$  content was 1.42–3.33 and 1.10–3.76 times higher than the drinking water quality safe limit of 300 mg/L (BIS 2012) in 95.45% of both the pre- and post-monsoon groundwater samples (2–22), respectively (Fig. 1). The carbonates and bicarbonates prompt the increment of pH and calcareousness of soil. This is the detrimental factor for plants as the greater part of it can't develop well. As a result, the application of carbonated water will tend the soil to get the saline. Such soils will be destructive for development of plants (Bauder et al. 2014).

The concentration of  $\text{Cl}^-$  ranged from 21 to 808 mg/L with a mean value of 252.68 mg/L in the pre-monsoon groundwater and 256 mg/L in the post-monsoon groundwater (Table 3; Fig. 3). This is a nonlithological source (Subba Rao 2017). Dry climate, domestic wastes, septic tank, leakages, and irrigation-return-flows are the important sources of  $\text{Cl}^-$  in the groundwater (Subba Rao 2020). The contribution of  $\text{Cl}^-$  to the total anions was 34.08% in the pre-monsoon groundwater and 33.99% in the post-monsoon groundwater (Table 3). The concentration of  $\text{Cl}^-$  in 45.45% of the groundwater samples (3, 4, 6, 8, 9, 11, 12, 14, 19, and 21) of the pre-monsoon period and 31.82% of the groundwater samples (2–4, 8, 9, 16, and 20) of the post-monsoon period exceeded the standard limit (250 mg/L) prescribed for portable water. It was 1.14–3.47 and 1.30–3.06 times more than the drinking water quality standard limit, which causes salty taste and laxative impacts (WHO 2017). Like  $\text{Na}^+$ , high  $\text{Cl}^-$  content causes more problems, when applied with sprinkler irrigation (Bauder et al. 2014). Although it is a common anion in the irrigation water, it is an essential for plants in low amounts. However, if it is in high concentration, it reduces the crop yields.

In the present study area, the concentration of  $\text{SO}_4^{2-}$  was in between 0.58 and 403 with a mean value of 106.28 mg/L in the pre-monsoon groundwater (Table 3; Fig. 3), which contributed 10.56% to the total anions, and 93 mg/L in the post-monsoon groundwater, which contributed 9.13% of total anions. Gypsum used to alter the physical properties of soil conditions is the primary source of  $\text{SO}_4^{2-}$  content in the groundwater (Subba Rao 2020), because no sulphide-bearing mineral deposits present in the country rocks. The concentration of  $\text{SO}_4^{2-}$  was 1.25–2.02 and 1.87–1.88 times higher than the safe limit of 200 mg/L prescribed for drinking water (BIS 2012) in 13.64% of the pre-monsoon groundwater samples (8, 9, and 14) and 9.09% of the post-monsoon groundwater samples (9 and 20), respectively (Fig. 1),

causing the bitter taste (WHO 2017). The  $\text{SO}_4^{2-}$  is a major contributor to increase the salinity in the irrigation water, which contributes to soil fertility (Bauder et al. 2014). However, the irrigation water with  $\text{SO}_4^{2-}$  more than 400 mg/L reduces the phosphorus availability to plants.

The  $\text{NO}_3^-$ , which is the most oxidized state of nitrogen, has a nonlithological origin, such as sewage wastes, spillage of septic tanks, and agricultural fertilizers (Zhang et al. 2018; He et al. 2019). Therefore, the higher  $\text{NO}_3^-$  content in the groundwater is mainly related to anthropogenic source (Subba Rao 2017). The  $\text{NO}_3^-$  content was from 1.20 to 719 mg/L in the pre- and post-monsoon periods with a mean value of 90.70 and 199.60 mg/L, respectively (Table 3; Fig. 3). The contribution of  $\text{NO}_3^-$  to the total anions was 6.98% and 15.16% in the pre- and post-monsoon groundwater samples (Table 3). The  $\text{NO}_3^-$  content was 1.11–15.98 and 1.67–15.56 times more than the desirable limit of 45 mg/L recommended for drinking water (BIS 2012; WHO 2017) in 31.82% of the pre-monsoon groundwater samples (3, 4, 6, 8, 9, 14, and 21) and 59.09% of the post-monsoon groundwater samples (2–5, 8–10, 12, 13, 16, 17, 20, and 21), respectively (Fig. 1), which cause the blue baby disease (WHO 2017). The  $\text{NO}_3^-$  ion often occurs at higher concentrations than ammonium in the irrigation water (Bauder et al. 2014). High nitrogen water causes quality problems in certain crops, such as grain and sugar beets, and also causes to excess vegetative growth in some vegetables.

Fluoride-bearing minerals (biotite, hornblende, fluorite, and apatite) and phosphate fertilizers are the sources of  $\text{F}^-$  in the groundwater (Subba Rao et al. 2016, 2020a). In addition, Li et al. (2014) and Wu et al. (2015) also reported that  $\text{F}^-$ -rich groundwater, which recharges other aquifers, may also be important source. The values of  $\text{F}^-$  were in between 0.27 and 7.50 mg/L with a mean value of 3.23 mg/L in the pre-monsoon period and 1.72 mg/L in the post-monsoon period (Table 3; Fig. 3). The  $\text{F}^-$  contributed 0.82% and 0.43% to the total anions in the pre- and post-monsoon groundwater samples, respectively (Table 3). The concentration of  $\text{F}^-$  was 1.07–5.0 and 1.80–3.15 times more than the standard limit of 1.50 mg/L considered for drinking water (BIS 2012) in 68.18% of the pre-monsoon groundwater samples (2–5, 7–11, 13, 14, 16, 17, 20, and 21) and 31.82% of the post-monsoon groundwater samples (6–8, 11, and 18–20), respectively (Fig. 1). They lead to dental fluorosis (WHO 2017). The concentration  $\text{F}^-$  in the irrigation water effects the human health through the eating of leafs and vegetables, leading to spread of fluorosis (Mandal and Gupta 2015).

## Groundwater Quality Suitability

Seasonally, the drinking groundwater quality index (DGQI) was computed (Eqs. 2 and 5), considering the

pH, TDS,  $\text{Ca}^{2+}$ ,  $\text{Mg}^{2+}$ ,  $\text{Na}^+$ ,  $\text{K}^+$ ,  $\text{HCO}_3^-$ ,  $\text{Cl}^-$ ,  $\text{SO}_4^{2-}$ ,  $\text{NO}_3^-$ , and  $\text{F}^-$  analysed from the groundwater of the present study area, whereas the irrigation groundwater quality index (IGQI) was calculated (Eqs. 6 and 12), taking the pH, EC,  $\text{SO}_4^{2-}$ , SAR, % $\text{Na}^+$ , RSC, PI, MR, and KR into consideration. The combinations of  $\text{Ca}^{2+}$ ,  $\text{Mg}^{2+}$ ,  $\text{Na}^+$ ,  $\text{K}^+$ , and  $\text{HCO}_3^-$  were expressed in terms of SAR, % $\text{Na}^+$ , RSC, PI, MR, and KR (Eqs. 6 and 11).

### Drinking Purpose

The computed values of DGQI were from 32.70 to 815.17 with a mean of 171.48 in the pre-monsoon groundwater samples and were in between 27.28 and 466.04 with a mean of 161.30 in the post-monsoon groundwater samples (Table 4). According to the DGQI, the groundwater quality can be classified as different grades: excellent quality (< 50), good quality (50–100), poor quality (100–200), very poor quality (200 and 300), and unsuitable quality (> 300) for drinking purpose. Taking this into account, the last three groundwater quality types can be considered to be vulnerable zones.

As indicated by DGQI, 4.55% (1, 18, 20, and 22), 27.27% (2, 13, 15, 18, 20, and 22), 50% (3–7, 10–12, 16, 17, and 19), 13.63% (8, 9, and 21), and 4.55% (14) in the pre-monsoon period, and 4.55% (1), 27.27% (6, 12, 14, 15, 17, and 22), 40.91% (5, 7, 10, 11, 13, 16, 18, and 19), 9.09% (2 and 20), and 18.18% (3, 4, 8, and 9) in the post-monsoon period represented the excellent, good, poor, very poor, and unsuitable groundwater quality types, respectively (Fig. 4). It suggested the decrease of poor and very poor groundwater quality samples from the pre- to post-monsoon periods and the increase of unsuitable groundwater quality samples from the pre- to post-monsoon periods. This could be caused by different sources of availability of geogenic

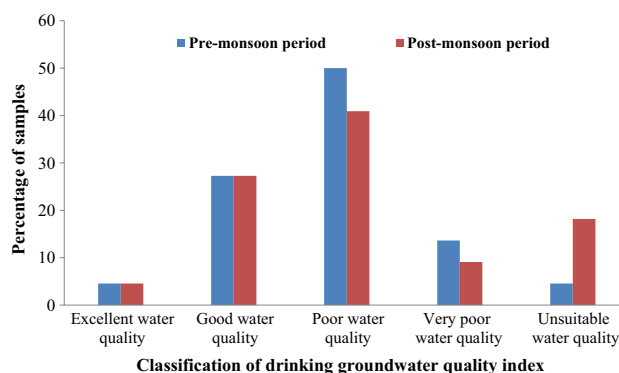


Fig. 4 Percentage of the groundwater samples based on the classification of drinking groundwater quality index (DGQI)

and anthropogenic origins, following the recharge of the groundwater.

Spatial distribution of DGQI is illustrated in Fig. 5. The areas of excellent, good, poor, very poor, and unsuitable groundwater quality zones were observed from 10.20%, 40.05%, 35.40%, 8%, and 6.35% in the pre-monsoon period and 15.86%, 30.63%, 40.13%, 11.26%, and 2.12% in the post-monsoon period. It suggested that the excellent, poor, and very poor groundwater quality zones were increased from the pre- to post-monsoon periods, whereas the poor and unsuitable groundwater quality zones were decreased in the post-monsoon period compared to the pre-monsoon period. As a whole, 49.75% and 54.51% of the vulnerable zones (poor, very poor, and unsuitable groundwater quality types) were observed from the pre- and post-monsoon periods, respectively. This difference is due to dilution of groundwater through the infiltration of various recharge water, following the topography.

The excellent and good groundwater qualities are suitable for drinking purpose, while the poor and very poor groundwater qualities are useful only for domestic purpose.

Table 4 Statistical summary of groundwater quality indices

Particulars	Pre-monsoon period (Pre)		Post-monsoon period (Post)		Arithmetic mean		Standard deviation		Coefficient of variation (%)	
	Min	Max	Min	Max	Pre	Post	Pre	Post	Pre	Post
Drinking groundwater quality index (DGQI)	32.70	815.70	27.28	466.04	171.48	161.30	170.34	114.05	99.34	70.71
Irrigation water quality parameters										
Sodium absorption ratio (SAR)	0.96	6.29	0.25	4.99	2.75	1.80	1.53	1.19	55.64	66.11
Percent sodium (% $\text{Na}^+$ )	8.76	20.69	3.24	10.82	14.33	10.09	3.08	3.60	21.49	35.68
Residual sodium carbonate (RSC)	20.40	115.42	23.08	219.78	79.13	90.06	24.44	40.58	30.89	45.06
Permeability index (PI)	6.93	12.61	4.40	11.20	9.91	7.67	1.51	1.73	15.24	22.56
Magnesium ratio (MR)	0.81	11.12	0.62	10.70	6.02	6.09	3.14	3.02	52.16	49.59
Keller ratio (KR)	10.11	52.11	2.68	39.57	26.78	14.58	13.10	9.31	48.92	63.85
Irrigation groundwater quality index (IGQI)	75.25	275.28	58.22	352.25	160.15	150.65	47.55	58.26	29.69	38.67

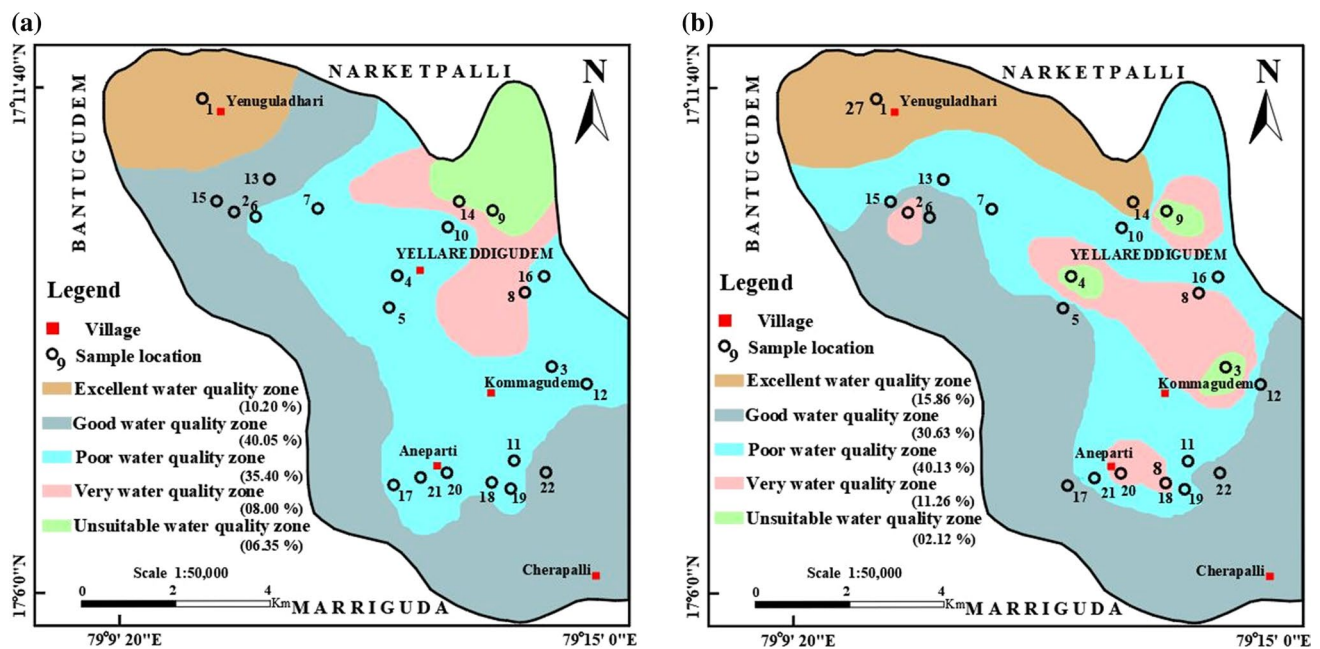


**Fig. 5** Seasonal and spatial distribution of the classification of drinking groundwater quality index (DGQI): **a** pre-monsoon period and **b** post-monsoon period

However, such water requires some primary treatment for its proper utilization. The occurrence of the groundwater in the unsuitable groundwater quality zone is unfit for any purpose. It can be utilized after taking the specific water treatment.

### Irrigation Purpose

For assessing the groundwater quality for irrigation purpose, the irrigation chemical parameters, i.e., pH, EC,  $\text{SO}_4^{2-}$ , SAR,  $\text{\%Na}^+$ , RSC, PI, MR, and KR, were widely used. Their computed values are presented in Tables 3 and 4. The classifications of these parameters are shown in Table 5. In the pre- and post-monsoon periods, the pH was less than 8.5 in all groundwater samples (except one sample 12 in the post-monsoon period), which was suitable for irrigation. High irrigation water with a pH may cause a nutritional imbalance (NSW 2011). As per the classification of the salinity hazard (EC), 4.55%, 59.09%, and 36.36% of the groundwater samples were determined as medium salinity (EC: 250 to 750  $\mu\text{S/cm}$ ), high salinity (EC: 750 to 2250  $\mu\text{S/cm}$ ) and very high salinity (EC: > 2250  $\mu\text{S/cm}$ ) hazard types, respectively, in the pre-monsoon period, whereas 4.55%, 54.54% and 40.91% of the groundwater samples fall in medium, high and very high salinity hazard types in the post-monsoon period. The  $\text{SO}_4^{2-}$  was less than 400 mg/L in all pre- and post-monsoon groundwater samples (except one sample 14 in the pre-monsoon period), which were suitable for irrigation. The SAR varied from 0.96 to 6.29 with a mean value of 2.75 in the pre-monsoon groundwater and

from 0.25 to 4.99 with a mean value of 1.80 in the post-monsoon groundwater. According to the range of SAR, the SAR was less than 10 (0.25–6.29) in all groundwater samples in both the seasons, which were classified as low sodium hazard type for irrigation purpose. The  $\text{\%Na}^+$  was observed to be 8.76% to 20.69% in the pre-monsoon period and 3.24% to 10.82% in the post-monsoon period with a mean of 14.33% and 10.09%, respectively. As indicated by  $\text{\%Na}^+$  used for irrigation purpose, the  $\text{\%Na}^+$  was less than 60% in all groundwater samples, which was suitable for irrigation. The classification of RSC suggested that all groundwater samples (20.40–219.78 meq/L) of both the seasons were not fit (RSC: > 2.50 meq/L) for irrigation purpose. The PI varied from 4.40 to 12.61%, which was less than 25%, in the pre- and post-monsoon groundwater samples so that they were unsuitable for irrigation use. According to the MR classification, all pre- and post-monsoon groundwater samples showed the MR from 0.62 to 11.12, which fall in the suitable category (MR: < 50) for irrigation purpose. The KR ranged from 2.68 to 52.11, which was more than 1.0 in both the seasons in all groundwater samples and thereby the groundwater samples were not good for irrigation.

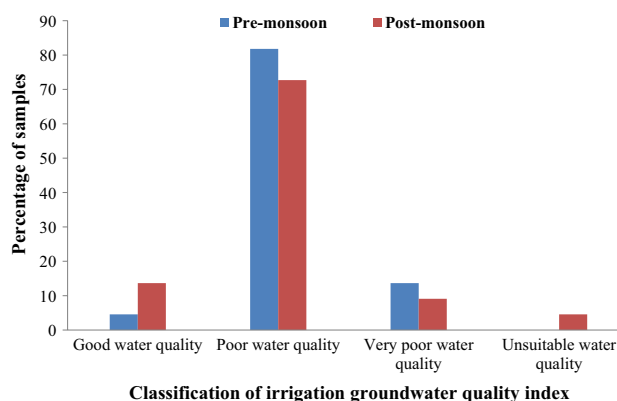
The overall groundwater quality for irrigation purpose is expressed in terms of IGQI, which were from 75.25 to 275.28 with a mean value of 160.15 in the pre-monsoon groundwater and were from 58.22 to 332.25 with a mean value of 150.65 in the post-monsoon groundwater (Table 4). According to the range of DGQI, the groundwater quality for irrigation purpose can also be classified into five types:

**Table 5** Classification of chemical parameters used for irrigation water quality assessment

Chemical parameters	Range	Pre-monsoon period		Post-monsoon period		Water quality
		Sample numbers	%	Sample numbers	%	
pH	< 8.5	1–11 and 13–22		1–11 and 13–22		Suitable
	> 8.5	12	4.55	12	4.55	Unsuitable
EC ( $\mu\text{S}/\text{cm}$ )	< 250	–	–	–	–	Low salinity hazard
	250–750	1	4.55	1	4.55	Medium salinity hazard
	750–2250	2, 4, 5, 7, 10, 12, 13, 15–18, 20, and 22	59.09	5–7, 10–12, 14, 15, 17, 19, 21, and 22	54.54	High salinity hazard
	> 2250	3, 6, 8, 9, 11, 14, 19, and 21	36.36	2–4, 8, 9, 13, 16, 18, and 20	40.91	Very high salinity hazard
$\text{SO}_4^{2-}$ (mg/L)	< 400	1–13 and 15–22		95.45		Suitable
	> 400	14	4.55	–	–	Unsuitable
	SAR	< 10	1–22	100	1–22	100
SAR	10–18	–	–	–	–	Medium sodium hazard
	18–26	–	–	–	–	High sodium hazard
	> 26	–	–	–	–	Very high sodium hazard
	%Na <sup>+</sup>	< 60	1–22	100	1–22	100
RSC (meq/L)	> 60	–	–	–	–	Unsuitable
	< 1.25	–	–	–	–	Suitable
	1.25–2.50	–	–	–	–	Marginal
PI (%)	> 2.50	1–22	100	1–22	100	Unsuitable
	< 25	1–22	100	1–22	100	Unsuitable
	25–75	–	–	–	–	Marginal
	75–100	–	–	–	–	Suitable
	> 50	–	–	–	–	Unsuitable
MR	< 50	1–22	100	1–22	100	Suitable
	> 50	–	–	–	–	Unsuitable
KR	< 1	–	–	–	–	Suitable
	> 1	1–22	100	1–22	100	Unsuitable

excellent quality if < 50; good quality if between 50 and 100; poor quality if varies from 100 to 200; very poor quality if ranges from 200 to 300; and unsuitable quality if exceeds 300 for irrigation purpose. The last three groundwater quality types can be treated to be vulnerable zones.

According to the classification of IGQI, 4.55% (1), 81.81% (2, 4–7, 9–13, and 15–22), and 13.64% (3, 8, and 14) of the groundwater samples in the pre-monsoon period were classified as good, poor, and very poor quality types, respectively (Fig. 6). In the post-monsoon period, 13.64% (1, 14, and 15), 72.72% (2, 3, 5–7, 10–13, and 16–22), 9.09% (4 and 8), and 4.55% (9) of the groundwater samples were classified as good, poor, very poor, and unsuitable quality types, respectively. The differences in the groundwater quality showed an increase of the good groundwater quality in a number of groundwater samples in the post-monsoon period compared with the pre-monsoon period. The unsuitable groundwater quality in the post-monsoon period was not observed from the pre-monsoon period. Furthermore, a number of groundwater samples of poor and very poor groundwater qualities were more in the pre-monsoon period

**Fig. 6** Percentage of the groundwater samples based on the classification of irrigation groundwater quality index (IGQI)

than in the post-monsoon period. As explained in the case of DGQI, the differences in the groundwater samples in IGQI could also be caused by variation in the geogenic and anthropogenic sources, following the groundwater recharge.



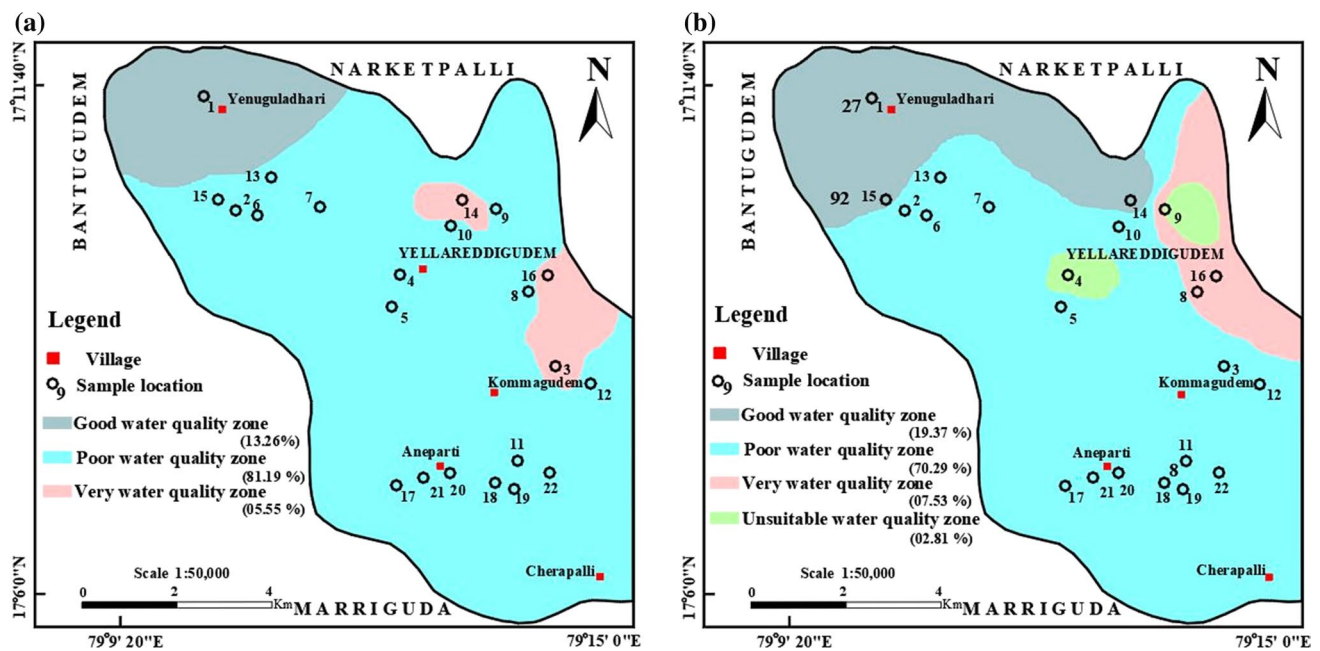


**Fig. 7** Seasonal and spatial distribution of the classification of irrigation groundwater quality index (IGQI)—**a** pre-monsoon period and **b** post-monsoon period

Figure 7 illustrates the spatial distribution of IGQI. As shown in Fig. 7, 13.26%, 81.19%, and 5.55% of the total present study area fall in the good, poor, and very poor groundwater quality zones in the pre-monsoon period, respectively, whereas the 19.37%, 70.29%, 7.53%, and 2.81% of the total area represented the good, poor, very poor, and unsuitable groundwater quality zones in the post-monsoon period, respectively. It was noted that the good, very poor, and unsuitable groundwater quality zones were increased, whereas the poor groundwater quality zone was decreased in the post-monsoon period compared with the pre-monsoon period. As a whole, 86.74% and 80.63% of the vulnerable zones were observed from the pre- and post-monsoon periods, respectively. The decrease of vulnerable zone from the pre- to post-monsoon periods may be caused by difference in the variation of dilution of groundwater through the infiltration of various recharge water, depending on the topographical features.

The occurrence of the groundwater in the good groundwater quality zone of the present study area is fit for irrigation purpose, whereas the poor and very poor groundwater qualities from the vulnerable zones are not suitable for irrigation purpose. However, this water may be used, after taking some preliminary treatment, such as adding gypsum for improvement of soil permeability. Although the groundwater in the unsuitable groundwater quality

zone is not fit for irrigation purpose, it can be used after specific treatment like improvement of drainage system, application of desalinization, etc. (Subba Rao 2017).

### Geochemistry of Groundwater

Geochemical facies, geochemical relations, Piper diagram, and principal component analysis were adopted to assess the factors controlling the groundwater quality (Subba Rao et al. 2002, 2012a, 2014, 2020b; Subba Rao and Surya Rao 2010; Subba Rao 2014, 2017; Deepali et al. 2015; 2019; Li et al. 2016a, 2016b; Wu et al. 2020).

### Geochemical Facies

Geochemical facies explained the distribution and genesis of significant groundwater types along the water flow-paths (Subba Rao et al. 2012a, 2012b; Subba Rao 2017). According to the percent ionic contribution (%), the order of dominant cations ( $\text{Ca}^{2+}$ ,  $\text{Mg}^{2+}$ ,  $\text{Na}^+$ , and  $\text{K}^+$ ) in the groundwater of the present study area was  $\text{Na}^+ > \text{Ca}^{2+} > \text{Mg}^{2+} > \text{K}^+$  in the pre- and post-monsoon (Table 3). The order of abundant anions ( $\text{HCO}_3^-$ ,  $\text{Cl}^-$ ,  $\text{SO}_4^{2-}$ ,  $\text{NO}_3^-$ , and  $\text{F}^-$ ) was  $\text{HCO}_3^- > \text{Cl}^- > \text{SO}_4^{2-} > \text{NO}_3^- > \text{F}^-$  in the pre-monsoon and  $\text{HCO}_3^- > \text{Cl}^- > \text{NO}_3^- > \text{SO}_4^{2-} > \text{F}^-$  in the post-monsoon.

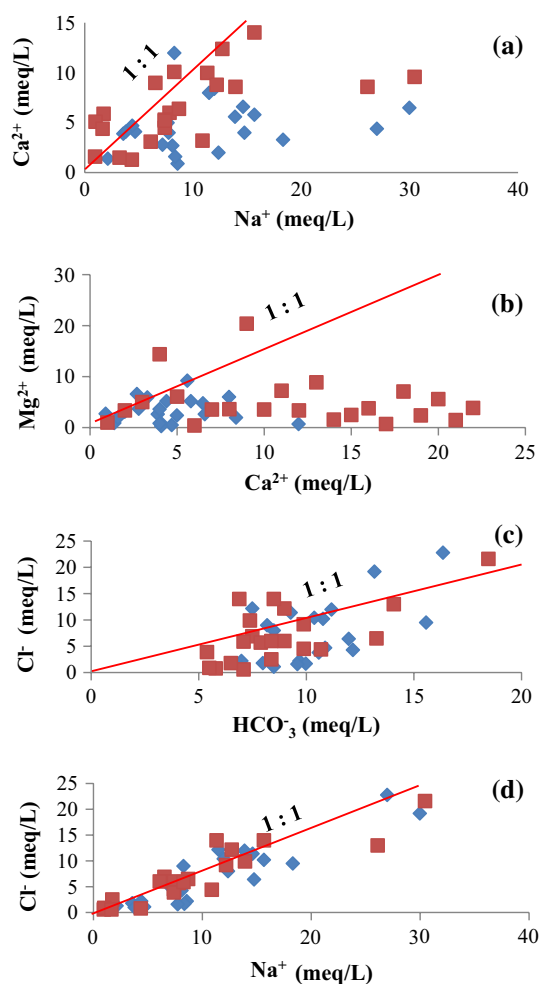
The area that was abundant by  $\text{HCO}_3^-$  ion in 81.82% of the groundwater samples (1–5, 7–11, 13, 15–20, and 22) is

classified as a recharge zone. The area that was dominant by  $\text{Cl}^-$  ion in 18.18% of the groundwater samples (6, 12, 14, and 21) reflects as a discharge zone (Subba Rao (2007). As shown in Figs. 1 and 2, the flow of groundwater was towards downstream (northwest) from upstream (southeast) and the majority of the groundwater samples showed the  $\text{HCO}_3^-$  as the dominant anion, which appear that most of the present study area comes under the recharge zone, following the topographical features. However, the change in the order dominance of anions from the pre-monsoon period ( $\text{HCO}_3^- > \text{Cl}^- > \text{SO}_4^{2-} > \text{NO}_3^- > \text{F}^-$ ) to the post-monsoon period ( $\text{HCO}_3^- > \text{Cl}^- > \text{NO}_3^- > \text{SO}_4^{2-} > \text{F}^-$ ) indicated the influence of surface contamination on the aquifer system due to higher contribution of  $\text{NO}_3^-$  in the post-monsoon period (15.16%) compared with the pre-monsoon period (6.98%; Table 3).

### Geochemical Relations

Geochemical relations were widely used to assess the origin of water through which it can be possible to evaluate the geochemical processes that results from the groundwater quality (Subba Rao et al. 2012a, 2012b; Li et al. 2016a, 2016b; Subba Rao 2017; Wu et al. 2020). Among the cations, the  $\text{Na}^+$  was the dominant ion (mean: 255.32 mg/L in the pre-monsoon period and 223 mg/L in the post-monsoon period; Table 3), which reflects the silicate weathering (Subba Rao et al. 2017). The concentration of  $\text{Na}^+$  (mean: 11.11 and 9.70 meq/L in the pre- and post-monsoon groundwater samples, respectively) was greater than that of  $\text{Ca}^{2+}$  (mean: 4.62 meq/L in the pre-monsoon period and 6.69 meq/L in the post-monsoon period; Fig. 8a), representing the ion exchange process (Subba Rao et al. 2019), whereas the concentration of  $\text{Ca}^{2+}$  (mean: 4.62 and 6.69 meq/L in the pre- and post-monsoon groundwater samples, respectively) was higher than that of  $\text{Mg}^{2+}$  (mean: 3.26 meq/L in the pre-monsoon period and 5.43 meq/L in the post-monsoon period; Fig. 8b), indicating the carbonate dissolution process in the groundwater system (Deepali et al. 2019). The low  $\text{K}^+$  content (mean: 0.36 meq/L in the pre-monsoon period and 0.16 meq/L in the post-monsoon period) among the cations is expected due to its higher resistance to chemical weathering of  $\text{K}^+$ -bearing minerals (orthoclase feldspars) and also its absorption on clay products (Subba Rao 2018).

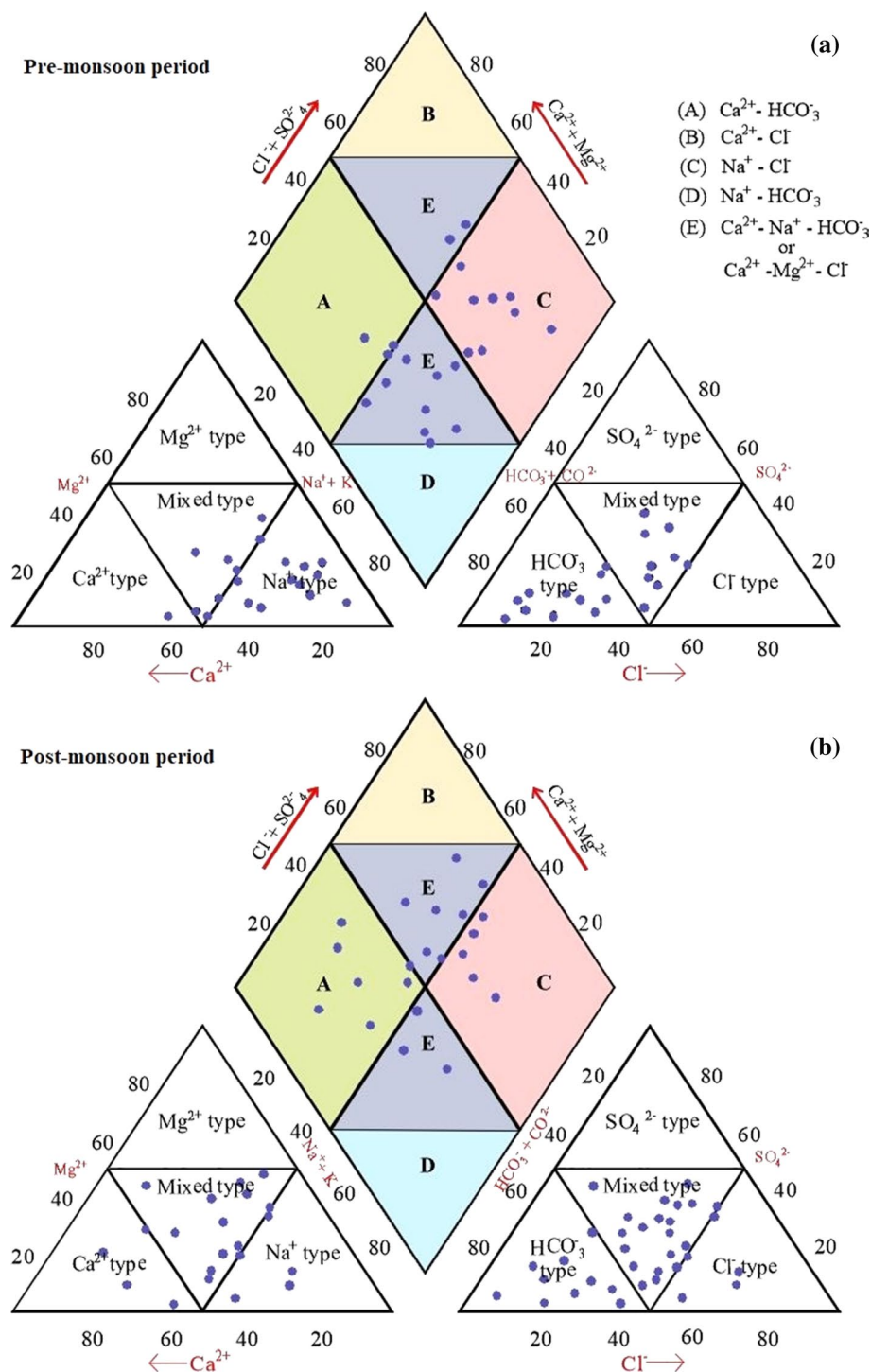
On the other hand, the dominance of  $\text{HCO}_3^-$  among the anions infers a mineral dissolution (Subba Rao et al. 2017). The higher  $\text{HCO}_3^-$  (mean: 9.95 and 8.77 meq/L) than the  $\text{Cl}^-$  (mean: 7.13 and 7.22 meq/L; Fig. 8c) in the pre- and post-monsoon groundwater samples reflects the mineral weathering (Subba Rao and Surya Rao 2010), while the higher  $\text{Na}^+$  (11.11 and 9.70 meq/L) than the  $\text{Cl}^-$  (mean: 7.13 and 7.22 meq/L; Fig. 8d) signifies the



**Fig. 8** Relationship between **a**  $\text{Na}^+$  and  $\text{Ca}^{2+}$ , **b**  $\text{Ca}^{2+}$  and  $\text{Mg}^{2+}$ , **c**  $\text{HCO}_3^-$  and  $\text{Cl}^-$ , and **d**  $\text{Na}^+$  and  $\text{Cl}^-$  Red and blue colors denote the pre- and post-monsoon, respectively

consequence of the rock weathering. Furthermore, the occurrence of calcium carbonate concretions in the soil cover reflects the prevailing conditions of dry climate (Subba Rao et al. 2019). Furthermore, the concentration of  $\text{NO}_3^-$  was 9.07–19.96 times (mean: 90.70–199.60 mg/L; Table 3) higher than its natural occurrence of 10 mg/L in the groundwater indicates the influence of anthropogenic source on the aquifer system (Subba Rao 2017). It also was significant to note that the higher  $\text{NO}_3^-$  content in the post-monsoon period (mean: 199.60 mg/L) than in the pre-monsoon period (mean: 90.70 mg/L) clearly specifies the impact of non-lithological sources, including household wastes, septic tank spillages, and nitrogen fertilizers through the leaching process.

From the observations of the above, it can be concluded that the sources of water and rock interactions associated with the rock-weathering and dissolution, leaching, ion

**Fig. 9** Geochemical characteristics of groundwater

exchange, and evaporation and also the sources of anthropogenic origin are the important controlling factors of the groundwater chemistry in the present study area.

#### Geochemical Characteristics of Groundwater

Piper diagram is an effective tool to classify the groundwater quality types on the basis of hydrogeochemical

characteristics (Piper 1944; Subba Rao 2017; He and Li 2019). It may be classified into five geochemical characteristics of the groundwater zones (Fig. 9). They are (a) carbonate hardness zone or temporary hardness zone or fresh water zone ( $\text{Ca}^{2+}$ - $\text{HCO}_3^-$ ), (b) noncarbonate hardness zone or permanent hardness zone ( $\text{Ca}^{2+}$ - $\text{Cl}^-$ ), (c) noncarbonate alkali zone or saline water zone ( $\text{Na}^+$ - $\text{Cl}^-$ ), (d) carbonate alkali zone or excess alkalinity zone ( $\text{Na}^+$ - $\text{HCO}_3^-$ ), and (e)

mixed water zone or transition zone ( $\text{Ca}^{2+}$ – $\text{Mg}^{2+}$ – $\text{Cl}^-$  and  $\text{Ca}^{2+}$ – $\text{Na}^+$ – $\text{HCO}_3^-$ ).

As observed from Fig. 9, 13.64% (7, 13, and 20), 40.91% (1, 4, 8, 9, 11, 14, 16, 19, and 21), and 45.45% (2, 3, 5, 6, 12, 10, 15, 17, 18, and 22) of the pre-monsoon groundwater samples and 31.82% (5, 7, 11, 14, 15, 18, and 22), 22.73% (8, 9, 16, 17, and 20), and 45.45% (2, 3, 4, 6, 7, 10, 12, 13, 19, and 21) of the post-monsoon groundwater samples fall in the carbonate hardness, noncarbonate alkali, and mixed groundwater zones, respectively. The dominance of carbonate hardness and mixed groundwater quality types reflect the silicate weathering associated with the dissolution, ion exchange, and evaporation factors, supporting the geochemical facies and processes (Subba Rao and Surya Rao 2010; Subba Rao et al 2017). Furthermore, the dominance of geochemical characteristics of groundwater zones in their decreasing order of percentage were mixed water > saline water > fresh water in the pre-monsoon period, while they were mixed water > fresh water > saline water in the post-monsoon period. This suggests that the increase of fresh groundwater quality by decreasing the saline groundwater quality from the pre- to post-monsoon periods is expected due to dilution of saline groundwater during monsoon.

### Principal Component Analysis

The principal component analysis (PCA) is a statistical method that provides a unique solution through the reconstruction of new results from the original data, with varimax rotated R-mode (Subba Rao 2014; Wu et al. 2014; Li et al. 2019c). As per the Kaiser Criterion, the principal components (PCs) were extracted with varimax rotation of loadings

for the maximum variance, which had eigenvalues more than one (Deepali et al. 2015). The TDS is a result of all ionic concentrations of  $\text{Ca}^{2+}$ ,  $\text{Mg}^{2+}$ ,  $\text{Na}^+$ ,  $\text{K}^+$ ,  $\text{HCO}_3^-$ ,  $\text{Cl}^-$ ,  $\text{SO}_4^{2-}$ ,  $\text{NO}_3^-$ , and  $\text{F}^-$  so that the PCA was performed, taking the ions only into account, whose combinations can give clear cut information on the geochemical processes. The results of PCA are presented in Table 6.

As shown in Table 6, the high positive loadings of  $\text{Cl}^-$  (0.960),  $\text{SO}_4^{2-}$  (0.936),  $\text{Na}^+$  (0.898),  $\text{NO}_3^-$  (0.796),  $\text{K}^+$  (0.788), and  $\text{HCO}_3^-$  (0.683) in the pre-monsoon period and  $\text{Cl}^-$  (0.982),  $\text{Na}^+$  (0.918),  $\text{NO}_3^-$  (0.895),  $\text{SO}_4^{2-}$  (0.803),  $\text{Mg}^{2+}$  (0.764),  $\text{HCO}_3^-$  (0.748), and  $\text{Ca}^{2+}$  (0.717) in the post-monsoon period of PC1 accounted for 55.128% and 55.995% of the total variance with an eigenvalue of 4.962 and 5.040, respectively. The combination of  $\text{Ca}^{2+}$ ,  $\text{Mg}^{2+}$ ,  $\text{Na}^+$ ,  $\text{K}^+$ , and  $\text{HCO}_3^-$  reflects the silicate weathering and dissolution (Eqs. 13 and 15), whereas those of  $\text{Cl}^-$ ,  $\text{SO}_4^{2-}$ , and  $\text{NO}_3^-$  measures the impact of surface contamination caused by domestic wastes, irrigation-returns-flows, and utilization of unlimited gypsum and nitrogenous fertilizers (Subba Rao et al. 2017, 2019). Waste waters and potassium fertilizers are the additional sources of  $\text{Mg}^{2+}$ ,  $\text{Na}^+$ ,  $\text{K}^+$ ,  $\text{Cl}^-$ , and  $\text{NO}_3^-$  in the groundwater system (Subba Rao 2014). Thus, the PC1 is considered the geogenic and anthropogenic activities as the contaminated source of the groundwater.

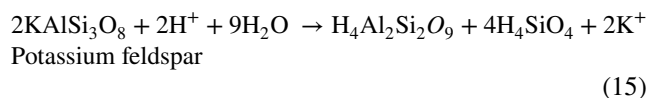
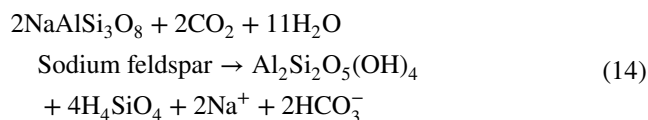
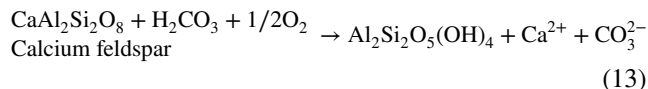


**Table 6** Principal component analysis (bold letters denote the high loadings > 0.75)

Particulars	Pre-monsoon period		Post-monsoon period	
	PC1	PC2	PC1	PC2
$\text{Ca}^{2+}$	0.431	<b>0.759</b>	<b>0.717</b>	-0.358
$\text{Mg}^{2+}$	0.577	-0.432	<b>0.764</b>	0.049
$\text{Na}^+$	<b>0.898</b>	-0.261	<b>0.918</b>	0.208
$\text{K}^+$	<b>0.788</b>	0.011	0.362	-0.288
$\text{HCO}_3^-$	<b>0.683</b>	-0.497	<b>0.748</b>	0.484
$\text{Cl}^-$	<b>0.960</b>	0.027	<b>0.982</b>	-0.046
$\text{SO}_4^{2-}$	<b>0.936</b>	0.193	<b>0.803</b>	0.100
$\text{NO}_3^-$	<b>0.796</b>	-0.140	<b>0.895</b>	-0.308
$\text{F}^-$	0.188	<b>-0.874</b>	0.004	<b>0.899</b>
Eigenvalue	4.962	1.798	5.040	1.406
Cumulative eigenvalue	4.962	6.670	5.040	6.446
Total variance (%)	55.128	19.974	55.995	15.626
Cumulative total variation (%)	55.128	75.102	55.995	71.621

In PC2, the  $\text{Ca}^{2+}$  showed the high positive loading (0.759) and the  $\text{F}^-$  had the high negative loading (-0.874) in the pre-monsoon period, and the  $\text{F}^-$  had the high positive loading (0.899) in the post-monsoon period, accounting for 19.974% and 15.626% of the total variance with an eigenvalue of 1.798 and 1.406, respectively (Table 6). The high loading of  $\text{Ca}^{2+}$  and high negative loading of  $\text{F}^-$  in the pre-monsoon period indicated that they are the origin of different sources. The F showed the high positive loading in the post-monsoon period, which is a consequence of impact of  $\text{F}^-$  minerals (hornblende, biotite, fluorite, and apatite) present in the host rocks and also phosphate fertilizers on the aquifer system (Subba Rao et al. 2016, 2020a). Thus, the PC2 is considered to be an indicative of  $\text{F}^-$  loading factor.

To study the combined controlling factors of PC1 and PC2 on the groundwater quality, the plot of ionic loadings



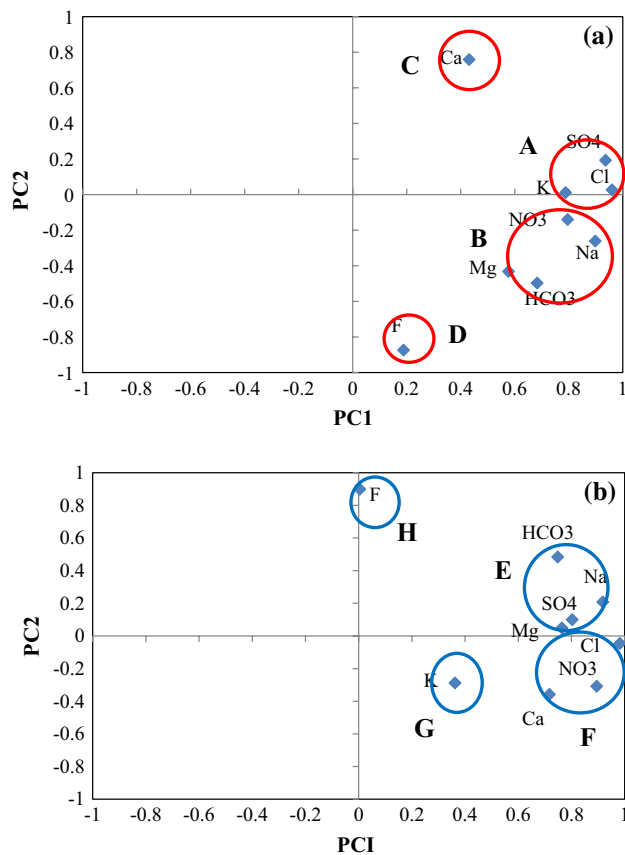


**Fig. 10** Relationship between PCI and PC2 with respect to **a** pre-monsoon period and **b** post-monsoon period

of PC1 versus PC2 is illustrated in Fig. 10, which were classified into groups, namely, A to D (pre-monsoon period) and E to H (post-monsoon period). As shown in Fig. 10, the Groups A ( $K^+$ ,  $Cl^-$ , and  $SO_4^{2-}$ ) and E ( $Mg^{2+}$ ,  $Na^+$ ,  $HCO_3^-$ , and  $SO_4^{2-}$ ) had positive factors of both PC1 and PC2. The PC1 showed a dominant influenced factor, but the PC2 was weak factor on both the groups. In case of the Groups B ( $Mg^{2+}$ ,  $Na^+$ ,  $HCO_3^-$ , and  $NO_3^-$ ) and F ( $Ca^{2+}$ ,  $Cl^-$ , and  $NO_3^-$ ), the impact of PC1 was a dominant factor, whereas that of PC2 was weak. Groups C ( $Ca^{2+}$ ) and H ( $F^-$ ) had positive influential factors of PC1 and PC2. However, the PC2 showed a dominant impact, whereas the PC1 had very weak impact. With respect to Groups D ( $F^-$ ) and G ( $K^+$ ), the impact of PC2 was noted factor, but the impact of PC1 was very weak. Consequently, the groups inferred that the Groups A, B, E, and F had the most influential factors of PC1, whereas the Groups C, D, G, and H had the second dominant factors of PC2.

Relatively, the higher loadings of ions in the post-monsoon period than in the pre-monsoon period indicate the leaching of ions from the source material through the processes of weathering, dissolution, ion exchange,

leaching, and evaporation as the dominant factors and also the influence of human interferences as the secondary factors that show the variation in the groundwater quality (Table 3). Furthermore, the PCA supports the results of the geochemical relations and chemical characteristics of the groundwater, which control the quality of groundwater.

## Conclusions

Groundwater plays a significant role for drinking and irrigation purposes in the area of Yellareddygudem watershed of Telangana, India, due to shortage of surface water resource. Therefore, the present study area was focused on the seasonal and spatial variation of groundwater quality suitability, using drinking groundwater quality index (DGQI), irrigation groundwater quality index (IGQI), and geographical information system (GIS). An attempt had been made to assess the governing factors of groundwater quality, using geochemical facies and relations, Piper diagram, and principal component analysis. The following conclusions were summarized below:

- The prevailing hydrogeochemical facies of groundwater in the present study area was  $Na^+HCO_3^-$  in the pre- and post-monsoon periods. Geochemical relations, Piper diagram, and principal component analysis supported the weathering, dissolution, leaching, ion exchange, and evaporation as the primary factors, controlling the groundwater quality and the anthropogenic source as the secondary factor.
- Seasonal variation of the groundwater quality suggested that the TDS,  $Na^+$ ,  $K^+$ ,  $Cl^-$ ,  $SO_4^{2-}$ , and  $F^-$  were found to be within the drinking water quality standard limits in most of the groundwater samples in the post-monsoon period compared to that of  $Ca^{2+}$ ,  $Mg^{2+}$ , and  $NO_3^-$  in the pre-monsoon period, whereas the pH and  $HCO_3^-$  were more than the standards limits in most of the groundwater samples in both the seasons.
- The DGQI suggested that the poor and very poor groundwater quality samples were decreased and the unsuitable groundwater quality samples were increased in the post-monsoon period compared with the pre-monsoon period. The IGQI showed the increase of good and unsuitable groundwater quality samples and the decrease of poor and very poor groundwater quality samples in the post-monsoon period compared with the pre-monsoon period. This difference is a result of variation in the sources of geogenic and anthropogenic origins between the pre- and post-monsoon periods, following the groundwater recharge.
- The spatial increase of vulnerable zones (poor, very poor, and unsuitable groundwater qualities) in the drinking water area and the decrease in the irrigation

area from the pre- to post-monsoon periods may be a result of variation in the dilution of groundwater through the infiltration of various recharge water, following the topography.

- (e) The present study will help to identify the seasonal and spatial variation of groundwater quality vulnerable zones for civic authorities to take the remedial measures to improve the water quality.

**Acknowledgements** The authors are thankful to the Director, Central Ground Water Board, Southern Region, Hyderabad, India, for providing facilities to carry out the chemical analysis. They are thankful to the Editor-in-Chief and anonymous reviewers for their valuable and constructive suggestions to improve the manuscript in the present form.

**Funding** The present work did not receive any financial assistance from any funding agency.

## Compliance with Ethical Standards

**Conflict of interest** No conflict of interest to declare.

## References

- APHA (2012) Standard methods for the examination of water and wastewater. American Public Health Association, Washington, DC
- Ayadi Y, Mokadem N, Besser H, Redhaounia B, Khelifi F, Harabi S, Nasri T, Hamed Y (2018) Statistical and geochemical assessment of groundwater quality in Teboursook area (Northwestern Tunisian Atlas). *Environ Earth Sci* 77:349. <https://doi.org/10.1007/s12665-018-7523-2>
- Bauder TA, Waskom RM, Sutherland PL, Davis JG (2014) Irrigation water quality criteria. Colorado State University. Fact Sheet No. 0.506
- BIS (2012) Indian Standard drinking water specification. Bureau of Indian Standard, New Delhi, p 10500
- Brindha K, Rajesh R, Murugan R, Elango L (2011) Fluoride contamination in groundwater in parts of Nalgonda district, Andhra Pradesh, India. *Environ Monit Assess* 172:481–492. <https://doi.org/10.1007/s10661-010-1348-0>
- CGWB (2015) Groundwater quality scenario in India. Central Ground Water Board, Government of India, New Delhi
- Deepali M, Malpe DB, Subba Rao N (2015) Identification of controlling processes of groundwater quality in a developing urban area using principal component analysis. *Environ Earth Sci* 74:5919–5933. <https://doi.org/10.1007/s12665-015-4616-z>
- Deepali M, Deepak DB, Subba Rao N (2019) Applications of geochemical and multivariate statistical approaches for the evaluation of groundwater quality and human health risks in a semi-arid region of eastern Maharashtra, India. *Environ Geochem Health*. <https://doi.org/10.1007/s10653-019-00478-1>
- Dinakar A (2018) Geochemical mechanisms of fluoride in groundwater and associated health risks in a part of Nalgonda district, Telangana state, India. Ph.D. thesis submitted to Andhra University, Visakhapatnam, India.
- Domenico PA, Schwartz FW (1990) Physical and chemical hydrogeology. Wiley, New York, NY
- Doneen LD (1964) Notes on water quality in agriculture. Published as a water science and engineering paper, 4001, Department of water science and engineering, University of California
- Eaton FM (1950) Significance of carbonates in irrigation waters. *Soil Sci* 39:123–133
- El Alfy M, Lashin A, Al-Arifi N, Al-Bassam A (2015) Groundwater characteristics and pollution assessment using integrated hydrochemical investigations GIS and multivariate geostatistical techniques in arid areas. *Water Resour Manag* 29:5593–5612. <https://doi.org/10.1007/s11269-015-1136-2>
- Franklin WT, Olsen JS, Soltanpour PN (2008) Effects of excessive magnesium in irrigation waters on wheat and corn growth. *Commun Soil Sci Plant Anal* 22:49–61. <https://doi.org/10.1080/00103629109368394>
- Freeze RA, Cherry JA (1979) Groundwater. Prentice-Hall, New Jersey
- He S, Li P (2019) A MATLAB based graphical user interface (GUI) for quickly producing widely used hydrogeochemical diagrams. *Geochemistry*. <https://doi.org/10.1016/j.chemer.2019.125550>
- He S, Wu J (2019a) Relationships of groundwater quality and associated health risks with land use/land cover patterns: a case study in a loess area, northwest China. *Hum Ecol Risk Assess* 25(1–2):354–373. <https://doi.org/10.1080/10807039.2019.1570463>
- He S, Wu J (2019b) Hydrogeochemical characteristics, groundwater quality and health risks from hexavalent chromium and nitrate in groundwater of Huanhe Formation in Wuqi County, northwest China. *Expo Health* 11(2):125–137. <https://doi.org/10.1007/s12403-018-0289-7>
- He X, Wu J, He S (2019) Hydrochemical characteristics and quality evaluation of groundwater in terms of health risks in Luohe aquifer in Wuqi County of the Chinese Loess Plateau, northwest China. *Hum Ecol Risk Assess* 25(1–2):32–51. <https://doi.org/10.1080/10807039.2018.1531693>
- Hem JD (1991) Study and interpretation of the chemical characteristics of natural water; U.S. Geological Survey Water Supply Paper 2254, p 264. Scientific Publishers, Jodhpur, India
- Ji Y, Wu J, Wang Y, Elumalai V, Subramani T (2020) Seasonal variation of drinking water quality and human health risk assessment in Hancheng City of Guanzhong Plain, China. *Expo Health* 12(3):469–485. <https://doi.org/10.1007/s12403-020-00357-6>
- Karunanidhi D, Aravinthasamy P, Priyadarsi DR, Praveenkumar RM, Prasanth K, Selvapraveen S, Thowbeekrahman A, Subramani T, Srinivasamoorthy K (2020) Evaluation of non-carcinogenic risks due to fluoride and nitrate contaminations in a groundwater of an urban part (Coimbatore region) of south India. *Environ Monit Assess* 192:102. <https://doi.org/10.1007/s10661-019-8059-y>
- Kelley WP (1940) Permissible composition and concentration of irrigation waters. *Proc Am Soc Civil Eng* 66:607–613
- Krishnakumar P, Lakshumanan C, Pradeep Kishore V, Sundararajan M, Santhiya G, Chidambaram S (2014) Assessment of groundwater quality in and around Vedaraniyam, South India. *Environ Earth Sci* 71:2211–2225. <https://doi.org/10.1007/s12665-013-2626-2>
- Kumar PR, Somashekar RK, Angami M (2010) Hydrochemistry and evaluation of groundwater suitability for irrigation and drinking purposes in the Markandeya River basin, Belgaum District, Karnataka State, India. *Environ Monit Assess* 173:459–487. <https://doi.org/10.1007/s10661-010-1399-2>
- Li P (2020) To make the water safer. *Expo Health* 12(3):337–342. <https://doi.org/10.1007/s12403-020-00370-9>
- Li P, Qian H (2018) Water resources research to support a sustainable China. *Int J Water Resour Dev* 34(3):327–336. <https://doi.org/10.1080/07900627.2018.1452723>
- Li R, Zhang J, Xin X (2013) Effect of poor quality irrigation water on potassium release from soils under long-term fertilization. *Acta Agric Scand* 64:45–55. <https://doi.org/10.1080/09064710.2014.884158>

- Li P, Qian H, Wu J, Chen J, Zhang Y, Zhang H (2014) Occurrence and hydrogeochemistry of fluoride in shallow alluvial aquifer of Weihe River, China. *Environ Earth Sci* 71(7):3133–3145. <https://doi.org/10.1007/s12665-013-2691-6>
- Li P, Wu J, Qian H (2016) Hydrochemical appraisal of groundwater quality for drinking and irrigation purposes and the major influencing factors: a case study in and around Hua County, China. *Arab J Geosci* 9(1):15. <https://doi.org/10.1007/s12517-015-2059-1>
- Li P, Zhang Y, Yang N, Jing L, Yu P (2016) Major ion chemistry and quality assessment of groundwater in and around a mountainous tourist town of China. *Expo Health* 8(2):239–252. <https://doi.org/10.1007/s12403-016-0198-6>
- Li P, Tian R, Xue C, Wu J (2017) Progress, opportunities and key fields for groundwater quality research under the impacts of human activities in China with a special focus on western China. *Environ Sci Pollut Res* 24(15):13224–13234. <https://doi.org/10.1007/s11356-017-8753-7>
- Li P, He S, Yang N, Xiang G (2018) Groundwater quality assessment for domestic and agricultural purposes in Yan'an City, northwest China: implications to sustainable groundwater quality management on the Loess Plateau. *Environ Earth Sci* 77(23):775. <https://doi.org/10.1007/s12665-018-7968-3>
- Li P, Wu J, Tian R, He S, He X, Xue C, Zhang K (2018) Geochemistry, hydraulic connectivity and quality appraisal of multilayered groundwater in the Hongdunzi coal mine, Northwest China. *Mine Water Environ* 37(2):222–237. <https://doi.org/10.1007/s10230-017-0507-8>
- Li P, He X, Guo W (2019) Spatial groundwater quality and potential health risks due to nitrate ingestion through drinking water: a case study in Yan'an City on the Loess Plateau of northwest China. *Hum Ecol Risk Assess* 25(1–2):11–31. <https://doi.org/10.1080/10807039.2018.1553612>
- Li P, He X, Li Y, Xiang G (2019) Occurrence and health implication of fluoride in groundwater of loess aquifer in the Chinese Loess Plateau: a case study of Tongchuan, Northwest China. *Expo Health* 11(2):95–107. <https://doi.org/10.1007/s12403-018-0278-x>
- Li P, Tian R, Liu R (2019) Solute Geochemistry and Multivariate Analysis of Water Quality in the Guohua Phosphorite Mine, Guizhou Province, China. *Expo Health* 11(2):81–94. <https://doi.org/10.1007/s12403-018-0277-y>
- Lu C, Guo F, Yan Q, Zhang Z, Li D, Wang L, Zhou Y (2019) Hydrothermal synthesis of type II ZnIn<sub>2</sub>S<sub>4</sub>/BiPO<sub>4</sub> heterojunction photocatalyst with dandelion-like microflower structure for enhanced photocatalytic activity under simulated solar light degradation of tetracycline. *J Alloys Compd* 811:151976. <https://doi.org/10.1016/j.jallcom.2019.151976>
- Mondal D, Gupta S (2015) Influence of fluoride contaminated irrigation water on biochemical constituents of different crops and vegetables with an Implication to human risk through diet. *J Mater Environ Sci* 6(11):3134–3142
- Narsimha A (2020a) Controlling factors and mechanism of groundwater quality variation in semiarid region of South India: an approach of water quality index (WQI) and health risk assessment (HRA). *Environ Geochem Health* 42:1725–1752. <https://doi.org/10.1007/s10653-019-00374-8>
- Narsimha A (2020b) Spatial distribution, exposure, and potential health risk assessment from nitrate in drinking water from semi-arid region of South India. *Hum Ecol Risk Assess* 26:310–314. <https://doi.org/10.1080/10807039.2018.1508329>
- NSW (2011) Irrigation water quality. NSW Government, Department of primary industries, Sydney
- Omonona OV, Amah JO, Olorunju SB, Waziri SH, Ekwe AC, Umar DN, Olofinlade SW (2019) Hydrochemical characteristics and quality assessment of groundwater from fractured Albian carbonaceous shale aquifers around Enyigba-Ameri, southeastern Nigeria. *Environ Monit Assess* 191(3):125. <https://doi.org/10.1007/s10661-019-7236-3>
- Piper AM (1944) A graphical procedure in the geochemical interpretation of water analysis. *Trans Am Geophys Union* 25:914–928
- Ramachandran A, Sivakumar K, Shanmugasundharamc A, Sangunathan U, Krishnamurthy RR (2020) Evaluation of potable groundwater zones identification based on WQI and GIS techniques in Adyar River basin, Chennai, Tamilnadu, India. *Acta Ecol Sin.* <https://doi.org/10.1016/j.chnaes.2020.02.006>
- Şener Ş, Şener E, Davraz A (2017) Evaluation of water quality using water quality index (WQI) 544 method and GIS in Aksu River (SW-Turkey). *Sci Total Environ* 584:131–144. <https://doi.org/10.1016/j.scitotenv.2017.01.102>
- Su Z, Wu J, He X, Elumalai V (2020) Temporal changes of groundwater quality within the groundwater depression cone and prediction of confined groundwater salinity using Grey Markov model in Yinchuan area of northwest China. *Expo Health* 12(3):447–468. <https://doi.org/10.1007/s12403-020-00355-8>
- Subba Rao N (2007) Groundwater quality as a factor for identification of recharge zones. *Environ Geosci* 14:79–90. <https://doi.org/10.1306/eg.05030606003>
- Subba Rao N (2014) Spatial control of groundwater contamination, using principal component analysis. *J Earth Syst Sci* 123:715–728. <https://doi.org/10.1007/s12040-014-0430-3>
- Subba Rao N (2017) Hydrogeology: problems with solutions. Prentice Hall of India, New Delhi
- Subba Rao N (2018) Groundwater quality from a part of Prakasam district, Andhra Pradesh, India. *Appl Water Sci* 80:30. <https://doi.org/10.1007/s13201-018-0665-2>
- Subba Rao N (2020) Spatial distribution of quality of groundwater and probabilistic non-carcinogenic risk from a rural dry climatic region of South India. *Environ Geochem Health.* [https://doi.org/10.1007/s10653-020-00621-3\(012\)01234586](https://doi.org/10.1007/s10653-020-00621-3(012)01234586)
- Subba Rao N, Surya Rao P (2010) Major ion chemistry of groundwater in a river basin: a study from India. *Environ Earth Sci* 61:757–775. <https://doi.org/10.1007/s12665-009-0389-6>
- Subba Rao N, Prakasa Rao J, John Devadas D, Srinivasa Rao KV, Krishna C, Nagamalleswara Rao B (2002) Hydrogeochemistry and groundwater quality in a developing urban environment of a semi-arid region, Guntur, Andhra Pradesh. *J Geol Soc India* 59(2):159–166
- Subba Rao N, Subrahmanyam A, Ravi Kumar S, Srinivasulu N, Babu Rao G, Surya Rao P, Venktram Reddy G (2012) Geochemistry and quality of groundwater of Gummanampadu Sub-basin, Guntur District, Andhra Pradesh, India. *Environ Earth Sci* 67:1451–1471. <https://doi.org/10.1007/s12665-012-1590-6>
- Subba Rao N, Surya Rao P, Venktram Reddy G, Nagamani M, Vidyasagar G, Satyanarayana NLVV (2012) Chemical characteristics of groundwater and assessment of groundwater quality in Varaha River Basin, Visakhapatnam district, Andhra Pradesh, India. *Environ Monit Assess* 184:5189–5214. <https://doi.org/10.1007/s10661-011-2333-y>
- Subba Rao N, Vidyasagar G, Surya Rao P, Bhanumurthy P (2014) Assessment of hydrogeochemical processes in a coastal region: application of multivariate statistical model. *J Geol Soc India* 84:494–500. <https://doi.org/10.1007/s12594-014-0155-6>
- Subba Rao N, Dinakar A, Surya Rao P, Rao PN, Madhnure P, Prasad KM, Sudarshan G (2016) Geochemical processes controlling fluoride-bearing groundwater in the granitic aquifer of a semi-arid region. *J Geol Soc India* 88:350–356. <https://doi.org/10.1007/s12594-016-0497-3>
- Subba Rao N, Deepali M, Dinakar A, Chandana I, Sunitha B, Ravindra B, Balaji T (2017) Geochemical characteristics and controlling factors of chemical composition of groundwater in a part of Guntur district, Andhra Pradesh, India. *Environ Earth Sci* 76:747. <https://doi.org/10.1007/s12665-017-7093-8>

- Subba Rao N, Sunitha B, Rambabu R, Nageswara Rao PV, Surya Rao P, Deepthi Spandana B, Sravanthi M, Deepali M (2018) Quality and degree of pollution of groundwater, using PIG from a rural part of Telangana State, India. *Appl Water Sci* 8:227. <https://doi.org/10.1007/s13201-018-0864-x01789>
- Subba Rao N, Srihari C, Deepthi Spandana B, Sravanthi M, Kamalesh T, Jayadeep VA (2019) Comprehensive understanding of groundwater quality and hydrogeochemistry for the sustainable development of sub-urban area of Visakhapatnam, Andhra Pradesh, India. *Hum Ecol Risk Assess*. <https://doi.org/10.1080/10807039.2019.1571403>
- Subba Rao N, Ravindra B, Wu J (2020) Geochemical and health risk evaluation of fluoride rich groundwater in Sattenapalle region, Guntur district, Andhra Pradesh, India. *Hum Ecol Risk Assess*. <https://doi.org/10.1080/10807039.2019.1571403>
- Subba Rao N, Sunitha B, Adimalla N, Chaudhary M (2020) Quality criteria for groundwater use from a rural part of Wanaparthy District, Telangana State, India, through ionic spatial distribution (ISD), entropy water quality index (EWQI) and principal component analysis (PCA). *Environ Geochem Health* 42:579–599. <https://doi.org/10.1007/s10653-019-00393-5>
- Szaboles I, Darab C (1964) The influence of irrigation water of high sodium carbonate content of soils. In: Proceedings of 8th international congress of ISSS, trans, II, pp 803–812
- USSL (1954) Diagnosis and improvement of saline and alkali soils. United States Salinity Laboratory Handbook 60. US Department of Agriculture, New York
- Venkatramanan S, Chung SY, Ramkumar T, Rajesh R, Gnanachandrasamy G (2016) Assessment of groundwater quality using GIS and CCME WQI techniques: a case study of Thiruthuraiipoondi city in Cauvery deltaic region, Tamil Nadu, India. *Desalin Water Treat* 57(26):12058–12073. <https://doi.org/10.1080/19443994.2015.1048740>
- Wang L, Huang T, Yang G, Lu C, Dong F, Li Y, Guan W (2020) The precursor-guided hydrothermal synthesis of  $\text{CuBi}_2\text{O}_4/\text{WO}_3$  heterostructure with enhanced photoactivity under simulated solar light irradiation and mechanism insight. *J Hazard Mater* 381:120956–120967. <https://doi.org/10.1016/j.jhazmat.2019.120956>
- WHO (2017) Guidelines for drinking-water quality. World Health Organization, Geneva
- Wilcox LV (1955) Classification and use of irrigation waters. US Department of Agriculture, New York
- Wu J, Li P, Qian H, Duan Z, Zhang X (2014) Using correlation and multivariate statistical analysis to identify hydrogeochemical processes affecting the major ion chemistry of waters: case study in Laoheba phosphorite mine in Sichuan, China. *Arab J Geosci* 7(10):3973–3982. <https://doi.org/10.1007/s12517-013-1057-4>
- Wu J, Li P, Qian H (2015) Hydrochemical characterization of drinking groundwater with special reference to fluoride in an arid area of China and the control of aquifer leakage on its concentrations. *Environ Earth Sci* 73(12):8575–8588. <https://doi.org/10.1007/s12665-015-4018-2>
- Wu J, Zhou H, He S, Zhang Y (2019) Comprehensive understanding of groundwater quality for domestic and agricultural purposes in terms of health risks in a coal mine area of the Ordos basin, north of the Chinese Loess Plateau. *Environ Earth Sci* 78(15):446. <https://doi.org/10.1007/s12665-019-8471-1>
- Wu J, Li P, Wang D, Ren X, Wei M (2020) Statistical and multivariate statistical techniques to trace the sources and affecting factors of groundwater pollution in a rapidly growing city on the Chinese Loess Plateau. *Hum Ecol Risk Assess* 26(6):1603–1621. <https://doi.org/10.1080/10807039.2019.1594156>
- Yidana SM, Yidana A (2010) Assessing water quality using water quality index and multivariate analysis. *Environ Earth Sci* 59(7):1461–1473. <https://doi.org/10.1007/s12665-009-0132-3>
- Zhang Y, Wu J, Xu B (2018) Human health risk assessment of groundwater nitrogen pollution in Jinghui canal irrigation area of the loess region, northwest China. *Environ Earth Sci* 77(7):273. <https://doi.org/10.1007/s12665-018-7456-9>
- Zhou Y, Wei A, Li J, Yan L, Li J (2016) Groundwater quality evaluation and health risk assessment in the Yinchuan region, northwest China. *Expo Health* 8(3):443–456. <https://doi.org/10.1007/s12403-590016-0219-5>
- Zhou Y, Li P, Xue L, Dong Z, Li D (2020) Solute geochemistry and groundwater quality for drinking and irrigation purposes: a case study in Xinle City, North China. *Geochemistry*. <https://doi.org/10.1016/j.chemer.2020.125609>